

Rapid prey evolution and the dynamics of two-predator food webs

Stephen P. Ellner · Lutz Becks

Received: 25 March 2010 / Accepted: 23 September 2010 / Published online: 22 October 2010
© Springer Science+Business Media B.V. 2010

Abstract Traits affecting ecological interactions can evolve on the same time scale as population and community dynamics, creating the potential for feedbacks between evolutionary and ecological dynamics. Theory and experiments have shown in particular that rapid evolution of traits conferring defense against predation can radically change the qualitative dynamics of a predator–prey food chain. Here, we ask whether such dramatic effects are likely to be seen in more complex food webs having two predators rather than one, or whether the greater complexity of the ecological interactions will mask any potential impacts of rapid evolution. If one prey genotype can be well-defended against both predators, the dynamics are like those of a predator–prey food chain. But if defense traits are predator-specific and incompatible, so that each genotype is vulnerable to attack by at least one predator,

then rapid evolution produces distinctive behaviors at the population level: population typically oscillate in ways very different from either the food chain or a two-predator food web without rapid prey evolution. When many prey genotypes coexist, chaotic dynamics become likely. The effects of rapid evolution can still be detected by analyzing relationships between prey abundance and predator population growth rates using methods from functional data analysis.

Keywords Rapid evolution · Eco-evolutionary dynamics · Predator–prey · Consumer-resource · Cycles · Chaos · Chemostat

Introduction

Evolutionary changes in individual traits affecting population interactions often occur at the same time and at the same pace as ecological dynamics, with effects large enough to change the ecological dynamics (“eco-evolutionary dynamics”, Fussmann et al. 2007; Kinnison and Hairston 2007). Rapid changes of heritable traits in response to new or changing environmental conditions have now been observed in a broad range of species including bacteria, algae, terrestrial plants, birds, fishes, crustaceans, insects, lizards, and mammals (e.g., Hairston and Walton 1986; Reznick et al. 1997; Thompson 1998; Sinervo et al. 2000; Hendry et al. 2000; Cousyn et al. 2001; Reznick and Ghalambor 2001; Grant and Grant 2002; Hairston et al. 1999; Yoshida et al. 2003; Heath et al. 2003; Olsen et al. 2004; Gagneux et al. 2006; Duffy and Sivars-Becker 2007; Swain et al. 2007; Duffy et al. 2008; Kinnison et al. 2008; Tyerman et al. 2008; Kassen 2009). Ezard

Research supported by a grant from the James S. McDonnell Foundation and US National Science Foundation grant DEB-0813743. We dedicate this paper to Simon A. Levin, a pioneer in the study of eco-evolutionary dynamics, on the occasion of his 70th birthday.

Electronic supplementary material The online version of this article (doi:10.1007/s12080-010-0096-7) contains supplementary material, which is available to authorized users.

S. P. Ellner (✉) · L. Becks
Department of Ecology and Evolutionary Biology,
Cornell University, Ithaca, NY 14853-2701, USA
e-mail: spe2@cornell.edu

Present Address:

L. Becks
Department of General Ecology,
Zoological Institute, Centre for Biological Sciences,
University of Cologne, Cologne, Germany

et al. (2009) recently concluded that between-year phenotypic variation in heritable traits contributed at least as much as environmental variability to variation in population growth rates in four out of the five ungulate populations that they examined. Rapid evolution of one species can affect the abundance and behavior of other species in their community, creating a feedback loop between evolutionary and ecological processes. Palkovacs et al. (2009) found that evolution and co-evolution of fish species in Trinidadian streams had larger impacts than species invasion on some measures of ecosystem function.

Recent theoretical and experimental work has shown in particular that rapid evolution in a prey species can have major effects on the population dynamics of a predator–prey interaction (Abrams and Matsuda 1997; Abrams 2000; Yoshida et al. 2003, 2007; Jones and Ellner 2007). Figure 1 shows experimental results from a linear predator–prey food chain that we have been studying experimentally (Becks et al. 2010), with the rotifer, *Brachionus calyciflorus* as the predator and the green alga *Chlamydomonas reinhardtii* as

the prey. The “smoking gun” for the presence of eco-evolutionary dynamics is that predator and prey oscillations do not exhibit the quarter-period (or less) lag typical of consumer–resource cycles without evolution (Bulmer 1975). Rather, they cycle almost exactly out of phase with each other (Fig. 1a), as previously reported (Shertzer et al. 2002; Yoshida et al. 2003, 2007). This is impossible in a classical predator–prey model with total population abundances as the state variables, or in a chemostat model that also tracks the concentration of the limiting nutrient for prey growth, because it requires that trajectories cross: given the same amount of food at different times, the predators sometimes increase and sometimes decrease. Figure 1b shows that this occurs due to evolutionary change in prey vulnerability to predation. The prey defend against predation by forming clumps of cells too large for the predator to consume. This defense trait is heritable, with clumps of nine or more cells being nearly inedible (Becks et al. 2010, unpublished data). The edible and inedible prey cycle out of phase with each other, and the predator lags the edible prey by roughly a quarter period.

These findings, combined with the recent evidence for rapid evolution of ecologically important traits, suggest that contemporary rapid evolution may play a major role in the dynamics of ecological food webs. However, a simple predator–prey food chain takes diet specialization to the extreme: the predator has a one-item diet, and the prey face only one natural enemy. In real food webs, most species face multiple natural enemies—predators, parasites, or pathogens. Can rapid evolution still be a potent force in shaping the dynamics of more complex food webs?

In this paper we consider, as a starting point, the case where a prey species faces two potential predators. The evolution of prey traits conferring defense against predation then involves a potentially multidimensional tradeoff between defense against one predator, defense against the other predator, and other fitness components that are compromised either by the defense traits themselves (e.g., higher metabolic energy demand due to increased body size, or decreased nutrient uptake by an algal cell due to thicker cell walls), or by the resources required for defense traits. How does this multidimensional tradeoff affect the potential for rapid prey evolution, or the nature and magnitude of its expected effects on community dynamics? How are the resulting eco-evolutionary dynamics affected by the nature of the tradeoff: for example, whether the prey can evolve one general defense that deters all consumers to some degree, versus a situation where several specialized defenses are needed for each potential consumer, each with associated costs?

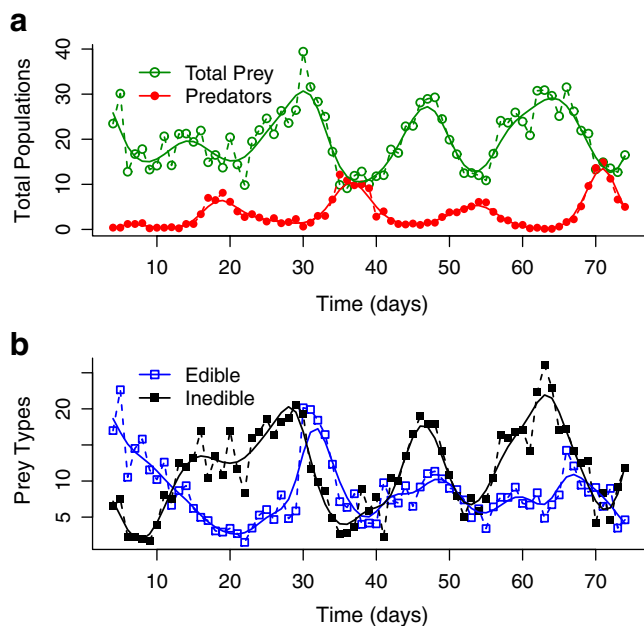


Fig. 1 Population and trait dynamics in experimental predator–prey chemostats (Becks et al. 2010 and L.B. Becks, unpublished data). **a** The predator (solid circles, red) is the rotifer *Brachionus calyciflorus*. The prey (open circles, green) is the green alga *Chlamydomonas reinhardtii*. Circles connected by dashed lines are the experimental data; the curves are smooths of the data by third-order local polynomial regression with data-driven bandwidth selection using the **locpol** package in R. **b** Edible (open squares, blue) and inedible (closed squares, black) algae. Algal cells in clumps of size 8 or smaller are classified as edible (Becks et al., unpublished data)

There is already a large theoretical literature on how evolution might affect population and community dynamics (e.g., Levin 1972; Levin and Udovic 1977; Doebeli and Koella 1995, 1996; Ferriere and Fox 1995; Khibnik and Kondrashov 1997; Johst et al. 1999; Abrams 2000; Zeineddine and Jansen 2005; Weitz et al. 2005; Dercole et al. 2006). What makes this paper different is the combination of two features. Firstly, evolutionary and ecological dynamics occur on the same time scale in our models, whereas most previous work has assumed a separation of time scales with evolution the slower process (e.g., evolution occurring through rare mutations, whose invasion fitness depends on the net effect of ecological processes averaged over many generations). Also, where previous literature has mostly focused on stability (i.e., whether evolution leads to stable equilibria, cycles, or chaos), our focus is on how ecological dynamics are altered by evolution occurring on the same time scale, phenomena that cannot occur when evolution occurs on a slower time scale (effects of rapid evolution on food web stability have been studied elsewhere (Abrams and Matsuda 1997; Tien 2010; Cortez and Ellner 2010); we return to this in the “Discussion”). We do not mean to imply that previous theory predicated on slow evolution is irrelevant. But rapid evolution is frequently observed, so it is also relevant to understand how rapid evolution can affect community dynamics.

The population dynamics in Fig. 1 are a “smoking gun” for eco-evolutionary dynamics because they cannot occur with strictly ecological dynamics. Our main question here is whether there are still distinctive properties of eco-evolutionary dynamics in more complex food webs, so that the dynamics of populations cannot be understood without taking into account the simultaneous evolution of those populations. We concentrate mainly on situations in which the dynamics are not chaotic. This is a reasonable assumption based on the available evidence, at least for terrestrial systems (Ellner and Turchin 1995), though the food web structures that we consider readily exhibit chaotic dynamics on the computer and in the laboratory (Becks et al. 2005; Benincà et al. 2008). But even without the possibility of chaos, our answer is “yes”: rapid prey evolution can give rise to distinctive patterns of food web dynamics that otherwise could not occur.

One-predator model

The models we study in this paper are based on a nondimensionalized model for one predator and two prey clones in a chemostat (Jones and Ellner 2007; Yoshida

et al. 2007). Because the prey reproduce asexually in our experimental system, they are represented in the model by a set of distinct clones, differing in their levels of defense against predation and their ability to compete for scarce nutrients. However, we show in Appendix A that our clone dynamics model (below) is mathematically equivalent to a gradient dynamics model for evolution of a quantitative trait in a sexually reproducing species, when only two prey clones can coexist in the long run, which is true in most of the cases we discuss below. Thus, many of our results will also be relevant to rapid evolution of quantitative defense traits in sexually reproducing prey species.

The model equations are

$$\begin{aligned}\dot{S} &= 1 - S - \sum_{i=1}^2 \frac{mSx_i}{k_i + S} \\ \dot{x}_i &= x_i \left[\frac{mS}{k_i + S} - \frac{gp_i y}{k_y + Q} - 1 \right] \\ \dot{y} &= y \left[\frac{gQ}{k_y + Q} - 1 \right]\end{aligned}\quad (1)$$

where $Q = \sum_i p_i x_i$. Here S is the limiting substrate, x_i are genotypes within the prey species that feed on the limiting substrate, and y is the predator. The cost for defense against predation (i.e., for having a low value of the predation risk p_i) is a higher value of the half-saturation constant for nutrient uptake, k_i . Time has been rescaled so that the chemostat dilution rate δ (the fraction of medium replaced each day) equals 1. One more rescaling can also be done to set $p_2 = 1$ without loss of generality ($k_b \rightarrow k_b/p_2$, $p_i \rightarrow p_i/p_2$). Table 1 (modified from Jones and Ellner 2007) gives values of the rescaled model parameters for two laboratory chemostat systems.

Figure 2 summarizes the predicted phase relations in the food-chain model when the prey population consists of two prey clones, one edible (x_2) and the other defended against predation (x_0). Figure 2a shows the structure of the food web, and Fig. 2b shows the analytically predicted phase relations. The circle, rotating counter-clockwise, represents the periodic orbit, with each species or genotype reaching its peak when it comes to the top of the circle. We have previously shown (Jones and Ellner 2007) that the prey and predator cycles are approximately out of phase with each other, as are the cycles of the edible and inedible prey types. A more refined prediction, derived in Appendix E.1, is that the prey types are not exactly out of phase. Rather, the undefended prey x_2 lags the defended prey x_0 by slightly less than half a period,

Table 1 Estimates of rescaled model parameters for predator–prey chemostat systems with the rotifer, *Brachionus calyciflorus* as the predator, and as prey either the green alga, *Chlorella vulgaris*, or the green alga, *Chlamydomonas reinhardtii*

Parameter	Description	Estimated values (<i>Chlorella</i> , <i>Chlamydomonas</i>)	Default values
m	Algal maximum per-capita population growth rate	$3.3/\delta$, $0.7/\delta$	$2/\delta$
k_2	Algal half-saturation constant for nutrient uptake, undefended prey	0.054, 0.014	0.03
g	Predator maximum population growth rate	$2.55/\delta$, $1.9/\delta$	$2.2/\delta$
k_y	Predator half-saturation constant for prey capture	0.21, 0.25	0.2

δ is the chemostat dilution rate. The rightmost column gives the parameter values used here for numerical solutions of the model, unless otherwise stated. *Chlorella* system estimates are from Jones and Ellner (2007) based on Yoshida et al. (2003, 2007), and *Chlamydomonas* system estimates are based on Becks et al. (unpublished data)

causing peaks of total prey abundance X to occur in between a peak of x_0 and a subsequent peak of x_2 . The predator y lags the undefended type x_2 by the classical quarter period. The result is that the predator is almost out of phase with total prey abundance, but not exactly, and predator peaks come slightly before troughs in the prey.

The analytic predictions in Fig. 2b, like all the others in this paper, were derived using several approximations. In particular, we analyze small fluctuations using linearization and then extrapolate to large fluctuations, and we assume that the prey genotypes are complete extremes, either completely undefended or almost perfectly defended, for reasons explained below (“Which prey types might coexist?”). The justification for these approximations is that they work—not just on the

computer (e.g., predicting what happens in numerical solutions such as Fig. 2c, d), but also in the laboratory. In Fig. 1b, the peaks in edible prey abundance slightly precede the troughs in inedible prey abundance, as predicted in Fig. 2d. Predators and total prey are also not exactly out of phase (Fig. 1)—predator troughs slightly precede the corresponding prey peak—but this difference is (as predicted) smaller than the peak-trough mismatch between the two prey types. The experimental support for these subtle predictions, all derived as analytic approximations, lend credibility to our predictions about more complex food webs that have yet to be tested experimentally.

Models with two predators

We now add a second predator z to model (1) in two different ways (see Fig. 3). In the first model, we add a second food chain in which the second predator z also has a separate and exclusive food supply W . We call this the *linked food chains* (LFC) model. In the second

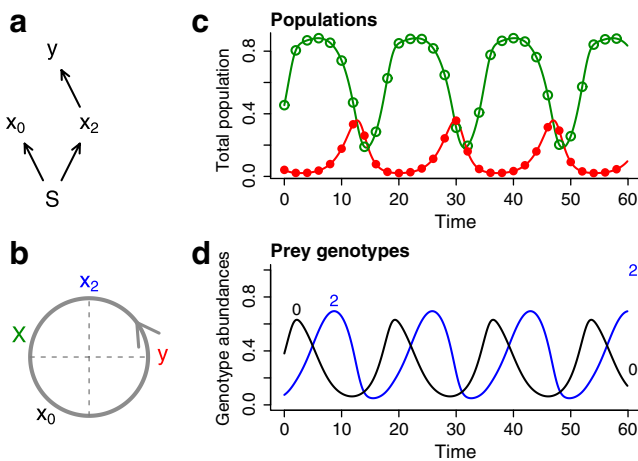


Fig. 2 Predicted phase relations and eco-evolutionary dynamics in a predator–prey food chain with edible and inedible prey genotypes. **a** Diagram of the food web **b** Predicted phase relations. **c, d** Population and genotype dynamics in numerical solutions of the model (predator: red, total prey: green, edible prey: blue, inedible prey: black). The numbers at the far right in **(d)** show the relative competitive abilities of the prey types, measured by $1/k_i$

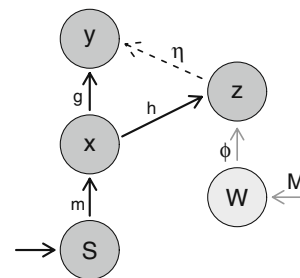


Fig. 3 Food webs with an additional predator z . S and W are externally supplied resources. The *solid black arrows* are always present, so that the focal prey species x has two predators. Adding the *solid grey arrows* creates the *linked food chains* (LFC) model. Adding instead the *dashed arrow* creates the *intermediate consumer* (IC) model. Symbols adjacent to arrows are the model parameter controlling the strength of that link. The model is scaled so that S is supplied at rate 1

model, we add instead intraguild predation: the second predator is consumed by the primary predator y . We call this the *intermediate consumer* (IC) model.

The reason for considering these models, rather than just adding the second predator, is to allow coexistence of two predators even when there is no genetic variation in the prey. Although nonequilibrium coexistence would still be possible without W or intraguild predation, our analyses assume small fluctuations, and non-equilibrium coexistence depends on large fluctuations. In the LFC model, steady-state coexistence is possible when z is the inferior competitor for x but persists because of the additional resource W . Steady-state coexistence is possible in the IC model when z is the better competitor for x , but predation by y keeps it in check.

In both the LFC and IC models, the trophic level of the second predator z is in between that of the x and y . We therefore refer to y as the *top* predator and z as the *intermediate* predator when talking about either model.

For simplicity we give z a type-I functional response on x and (in the LFC model) on its alternative food supply. This means that population oscillations are driven by the interaction between x and y . To describe the new predator in the LFC model, we introduce three new parameters: h is the grazing rate parameter for predation on x , M represents the (constant) supply rate of its food resource W , and ϕ is the grazing rate parameter for consumption of W . We let π_i denote the palatabilities of the two prey types to z , and define R to be the total x availability as perceived by z , $R = \sum_i \pi_i x_i$.

The equations for the LFC model are then

$$\begin{aligned} \dot{S} &= 1 - S - S \sum_i \frac{mx_i}{k_i + S} \\ \dot{x}_i &= x_i \left[\frac{mS}{k_i + S} - \frac{gp_i y}{k_y + Q} - h\pi_i z - 1 \right] \\ \dot{y} &= y \left[\frac{gQ}{k_y + Q} - 1 \right] \\ \dot{z} &= z [hR + \phi W - 1] \\ \dot{W} &= M - W - \phi z W \end{aligned} \tag{2}$$

These equations have already been put into the same scaling as the single-predator model, in the following sense: z is scaled so that a unit of algal consumption produces a unit of z , so z is also in units of substrate S , and W is scaled so that a unit consumption of W produces a unit of z .

Because the total prey density can be at most 1, a necessary condition for persistence of the intermediate

predator is $h + \phi M \geq 1$. Because $W \rightarrow M$ if the intermediate predator is absent, a sufficient condition for persistence of the intermediate predator is $\phi M > 1$.

In the IC model, z is characterized by h and by the grazing rate parameter, η , for y feeding on z , which is again assumed to be a type-I functional response. The model is then

$$\begin{aligned} \dot{S} &= 1 - S - S \sum_i \frac{mx_i}{k_i + S} \\ \dot{x}_i &= x_i \left[\frac{mS}{k_i + S} - \frac{gp_i y}{k_y + Q} - h\pi_i z - 1 \right] \\ \dot{y} &= y \left[\frac{gQ}{k_y + Q} + \eta z - 1 \right] \\ \dot{z} &= z [hR - \eta y - 1] \end{aligned} \tag{3}$$

As in the LFC model, $h > 1$ is necessary for persistence of the intermediate predator.

Results: dynamics without evolution

As the baseline for determining the effects of prey evolution in our two-predator food web models, we first analyze how the LFC and IC models behave when there is a single prey genotype that both predators can readily attack and consume. This section is really the most important in the paper. Numerical solutions can tell us how models behave when the prey are evolving, but to know that prey evolution is the cause of those behaviors, we have to know the limits to what is possible when the prey are not evolving.

The analysis uses a small-fluctuations approximation based on linearization at an equilibrium, and we used numerical simulations to verify the conclusions for large fluctuations. Appendix B explains how the calculations can be carried out using computer algebra, and Appendices C and D gives the results for the no-evolution scenarios. The conclusions, summarized in Figs. 4 and 5, are as follows.

In the LFC model (Fig. 4), the top predator y is linked only to the focal prey species x , so they exhibit classical consumer-resource cycles, with peaks in y lagging peaks in x by about a quarter period. The intermediate predator z also lags behind the focal prey species, but the lag is shorter because of its additional food resource W . When the intermediate predator is mainly dependent on the focal prey species x , the intermediate and top predators are nearly in phase.

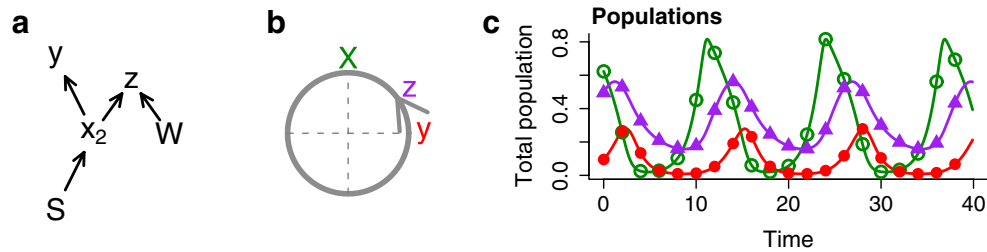


Fig. 4 Dynamics in the no-evolution baseline case of the linked food chains (LFC) model where the prey consists of one genotype x_2 vulnerable to attack by both predators.

However if the intermediate consumer mainly feeds on W rather than y , or if the cycle period is very long, the lag between the focal prey and the intermediate consumer can shrink to an arbitrarily small fraction of the cycle period. Numerical solutions of the model confirm this prediction (Appendix C).

In the IC model (Fig. 5), the linearized analysis predicts that the two predators should have lags on opposite sides of a quarter period, y longer and z shorter. When z is rare, so the side-chain is effectively absent, y 's lag behind the prey will be very close to a quarter period, and similarly if y is rare z 's lag will be nearly a quarter period. If neither predator is rare, there is a “tug of war” between the direct and indirect path from x to y . The former suggests a quarter-period lag, the latter suggests a half-period lag, and the outcome is a compromise. However, in order for cycles to occur the direct link must be strong, so for such parameters y 's lag is close to a quarter period while z 's lag is shorter.

Thus, without prey evolution there is a very limited range of possible dynamics for the LFC and IC models. Peaks of the top predator lag behind those of the focal prey species by about one quarter cycle period or slightly more, and peaks of the intermediate predator come somewhere in between those of the prey and the top predator.

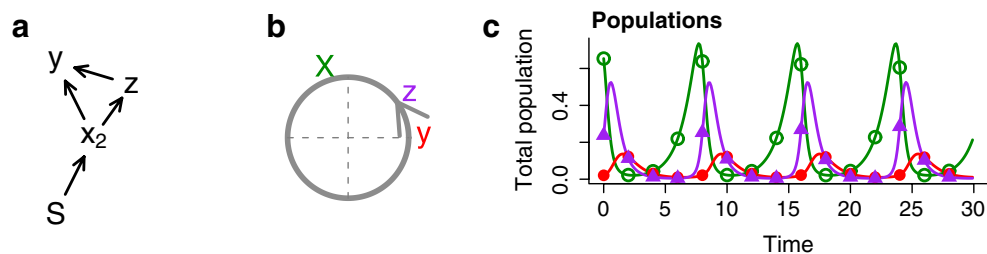


Fig. 5 Dynamics in the no-evolution baseline case of the Intermediate Consumer (IC) model where the prey consists of one genotype x_2 vulnerable to attack by both predators.

a–c are the same as in Fig. 2, with the addition of the second predator z (purple, solid triangles) in (c); as only one prey genotype is present, **d** is omitted

Results: eco-evolutionary dynamics with two predators

In this section we show that prey evolution greatly expands the range of dynamics that can occur in a two-predator food web, which is the main point of this paper. In “Which prey types might coexist?”, we show that coexisting prey types are typically extremes: either maximally or minimally defended against each predator. The food web dynamics then depend on which combination of genotypes is present, and in the rest of this section we consider the various possibilities. Table 2 summarizes the main findings, emphasizing the “smoking guns”—properties observable at the whole-population level, in one or both of our models, that can only occur when prey are evolving rapidly enough (on the time scale of a single population cycle) that the evolutionary dynamics can change the character of the ecological dynamics.

Which prey types might coexist?

To complete our eco-evolutionary models we, need to specify the set of competing prey genotypes. In this subsection, we state and justify our assumptions about the prey types.

Table 2 Combinations of coexisting prey genotypes that lead to eco-evolutionary dynamics, and key properties of the resulting food web dynamics

Description	Genotypes	Possible dynamics
Universal defense	x_0, x_2	Both predators “evolutionary”, cycling out of phase with total prey X .
Incompatible predator-specific defenses	x_y, x_z	(a) Total prey and total predators are out of phase, and the predators “take turns”: predator peaks are alternately dominated by y and by z . (b) Top predator out of phase with total prey, intermediate predator in phase with total prey.
Ignore the intermediate predator	x_2, x_z	(a) Top predator out of phase with total prey, intermediate predator “classical” (lags total prey by \approx one quarter period). (b) Top predator in phase with total prey, intermediate predator out of phase with total prey.
Free for all	x_2, x_y, x_z	Dynamics typically chaotic, with Q and R cycling out of phase, so that peaks of total predator abundance are alternately dominated by y and z .

Prey genotypes x_y, x_z, x_2, x_0 are vulnerable to predation by (respectively) only the top predator y , only the intermediate predator z , both predators, and neither predator. “Out of phase” denotes cycles such that maxima of one variable coincide with minima of the other, and vice versa; “in phase” means that maxima and minima of the two variables occur at the same time

Firstly, we assume that when multiple prey types coexist, they are extremes: both p and π are either the minimum or maximum values out of the assumed range of possible genotypes. The reason for this assumption is that whenever the tradeoff between the defense traits and k is linear, a noninvadable set of coexisting prey types (i.e., an evolutionarily stable combination (ESC)) must consist entirely of extreme types. This has been shown previously for coexistence at equilibrium (Jones and Ellner 2004), but it also applies to coexistence on a limit cycle or chaotic attractor, or if the system is subject to periodic, chaotic, or stationary stochastic forcing (Appendix F in the [Electronic supplementary material](#)).

The assumption that coexisting prey are extreme types will also be a reasonable approximation for some cases where the tradeoff curve is not completely linear, as in Fig. 6. The curve is drawn so that very effective defense ($0 < p \ll 1$) can be achieved at low cost, as is true in our *Chlorella* experimental system (Yoshida et al. 2004; Meyer et al. 2006), but complete invulnerability carries a high cost. Because the tradeoff curve is almost linear from $p = 1$ until p decreases to the “knee” (indicated by the dashed line in Fig. 6), the only the potential members of the ESC are the extreme types plotted as filled circles. This is not exact, because the better defended type in the ESC will not be exactly at the knee, but it is a good approximation because our models’ behaviors are not sensitive to small changes in a near-zero p or π value. When analyzing the models we assume that defense traits are 100% effective, so x_0 suffers no predation at all, but numerical solutions relax this assumption, as in Fig. 6, so both predators have a low but nonzero grazing rate on a defended genotype.

If the two defense traits p and π are free to vary independently, there can be up to four corner genotypes in the ESC: x_0 that neither predator can consume, x_2 that both can consume, x_y that only y can consume, and x_z that only z can consume. That allows $\binom{4}{2} + \binom{4}{3} + \binom{4}{4} = 11$ possible combinations of two or more persisting genotypes, each implying a different food web configuration at the genotype level. Considering each of these in turn would be tedious, and also unnecessary because the points we want to make about potential effects of rapid evolution can be made without being exhaustive. We therefore consider two mechanistically meaningful situations where the defense traits are coupled:

1. Universal defense: one trait defends against both predators. One example might be formation of

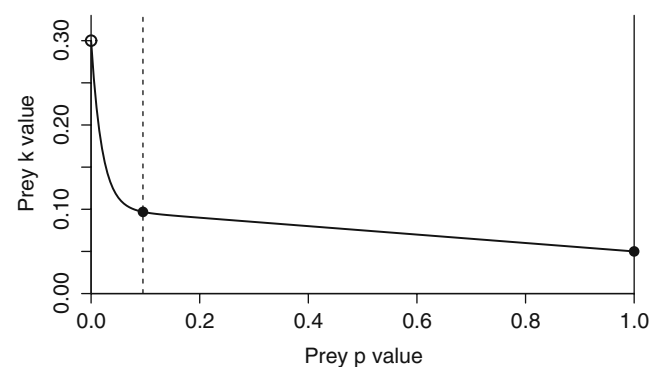


Fig. 6 Hypothetical tradeoff curve between prey palatability p and competitive ability k (with larger values of k meaning lower competitive ability when nutrients are scarce), such that an ESC can only include extreme types (indicated by filled circles): one at $p = 1$, the other at $p \approx 0$ just to the right of the knee in the tradeoff curve

clumps of cells by the prey (as in our *Brachionus-Chlamydomonas* experimental system) that are too large for either predator to consume. Other possible examples are a cryptic phenotype that all predators have trouble detecting, or a wide-spectrum toxin advertised by bright coloration.

- Incompatible predator-specific defenses: prey can defend against one or the other predator, or against neither, but not against both at once. This could occur due to an absolute incompatibility between traits, e.g., if coloration making the prey cryptic in one habitat makes it highly visible in another, or if a body size that is too large for one predator to handle is just right for the other. It also might occur if the cost of defending against both predators at once is prohibitively high.

The behavior of the LFC and IC models is often similar, because the models become nearly identical when z is strongly linked only to the focal prey x . As in the non-evolutionary scenarios, the main cause of differences between the models is the “tug of war” between the different phase relations favored by the direct and indirect chains from x to y .

Dynamics: universal defense trait

If one trait provides protection from both predators, the only possible ESC is the pair x_0, x_2 (Fig. 7 for the LFC model, and Fig. 13 in the [Electronic supplementary material](#) for the IC model, depicting results from Appendix E.2). Both predators are then driven by the oscillations of edible prey abundance, and have no links

to the inedible prey type. The x_2, y, z subsystem therefore acts like the complete food web of the corresponding no-evolution scenario. Specifically, the top predator lags the edible prey by a quarter period (or possibly a bit more in the IC model), and the intermediate predator is either in sync with the top predator or lags behind it by less than a quarter period. The inedible prey type x_0 cycles due to competition with the edible type, increasing when the edible type is driven to low numbers by predation and nutrients are plentiful, and decreasing when the edible type is abundant, nutrients are scarce, and the edible type is the superior competitor because it isn't paying a cost for defense. Because the two prey types cycle nearly (but not exactly) out of phase, the specialist predator oscillates nearly out of phase with total prey abundance, as in evolutionary cycles of the linear food chain.

Dynamics: incompatible predator-specific defense traits

The second and more interesting case of coupled defense traits is when prey can defend against one or the other predator, but not both. The possible ESC members are then x_y, x_z and x_2 , giving four possible combinations of two or more prey genotypes. However the combination (x_y, x_z) does not need to be considered, because in that case eco-evolutionary dynamics do not occur in our models. Both of these genotypes lack defense against the top predator, and the link to the top predator is the strong link driving cycles, so the genotypes cycle in near-synchrony. From the predators' perspective there is a single prey type with partial defense against z , so at the population level we observe classical consumer-resource dynamics.

Two defended genotypes If the cost of defense is low, the ESC will consist of the two defended types x_y, x_z . In that case, the outcome in the LFC model depends (as usual) on how strongly the intermediate predator feeds on the focal prey versus its alternative food source. If the intermediate predator feeds strongly on the focal prey species (Fig. 8, Appendix E.2), then each predator is driven by the prey genotype that it can consume, and lags this genotype by a quarter of the genotype's cycle period. The chains are only linked by prey competition for limiting substrate, so the two chains oscillate with the prey genotypes out of phase with each other. The resulting pattern at the population level is that peaks of total prey (each corresponding to a peak of one genotype) alternate with peaks of the predator populations, which are alternately one predator

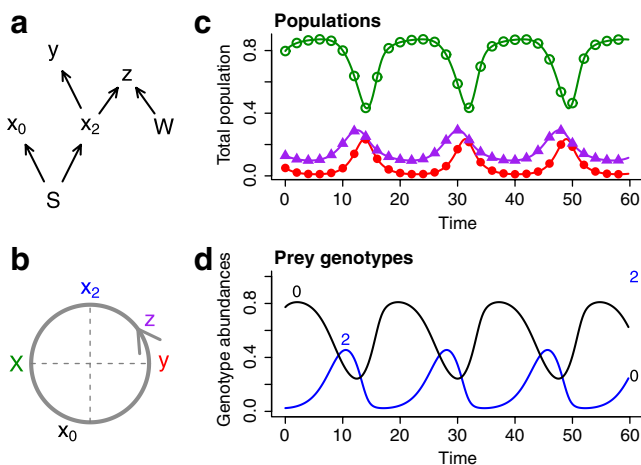


Fig. 7 LFC model when one trait confers effective defense against both predators ($p_1 = 0.05, \pi_1 = 0.1$), presented as in Fig. 2

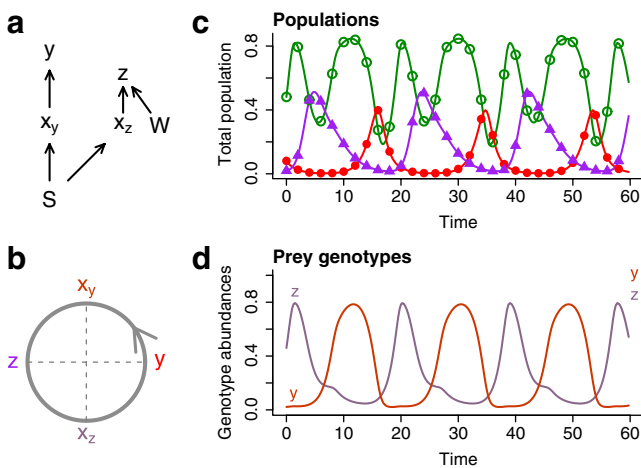


Fig. 8 LFC model with incompatible defenses: defense against one predator implies vulnerability to the other. Total prey X is not shown in (b) because its phase is not uniquely determined by the food web structure. The numerical solutions plotted here are for a case where the intermediate predator z exerts heavy grazing pressure on the focal prey x ($M = 1, \phi = 0.5, h = 2$), so an increase in z leads to a decrease in total prey abundance. In (d) recall that the labels y and z refer to the prey types x_y and x_z that are vulnerable to predation by the top predator y and intermediate predator z , respectively

and then the other. If the intermediate consumer feeds more heavily on its alternative food and less on x two changes can occur (Fig. 9): minima in x due to predation by the intermediate consumer can cease to occur, and

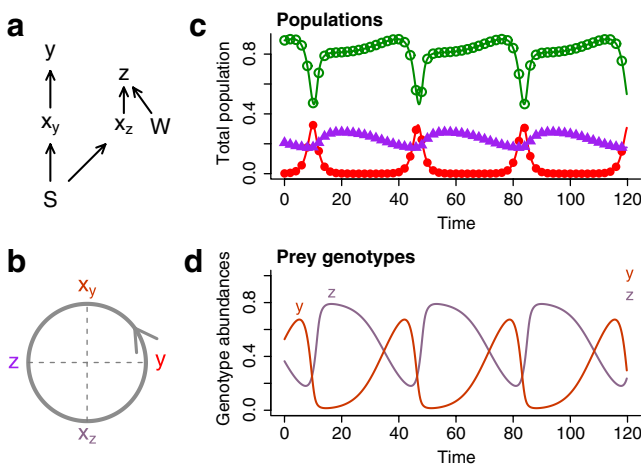


Fig. 9 LFC model dynamics with incompatible defenses as in Fig. 8, but with parameters such that the intermediate predator does not graze heavily on the focal prey x ($M = 0.2, \phi = 20, h = 0.5$). Total prey X is not shown in (b) because its phase is not uniquely determined by the food web structure

the lag between z and x_z (the genotype that it can consume) becomes very short. The population-level result is that the top predator cycles out-of-phase with total prey $X = x_y + x_z$, while the intermediate predator is nearly in sync with X .

The behavior of the IC model with the two defended types (Fig. 14 in the Electronic supplementary material) is very similar to Fig. 8. The only difference is that, due to the “tug of war” between the direct and indirect $x \leftrightarrow y$ links, y lags x_y by slightly more than a quarter period, while z lags x_z by slightly less. But at the population levels, the two models have the same qualitative behavior.

Ignore the intermediate The other possible two-type ESC consists of the two types x_2 and x_z with no defense against the intermediate predator z (Fig. 10). This situation could occur if z is too rare to be worth worrying about, if it doesn’t feed much on the focal prey species, or if the cost for defense against z is prohibitive.

In the LFC model, the two prey types are almost exactly out of phase, with defended type x_z lagging the edible type x_2 by slightly over half a cycle period (Fig. 10, Appendix E.2). Everything else follows from the food web structure and previous results. The top predator y lags its prey (x_2) by a quarter period, so it is nearly out of phase with total prey abundance X , as in basic evolutionary cycles (Fig. 2). For z , the two prey are equally edible, so it lags total prey abundance by a

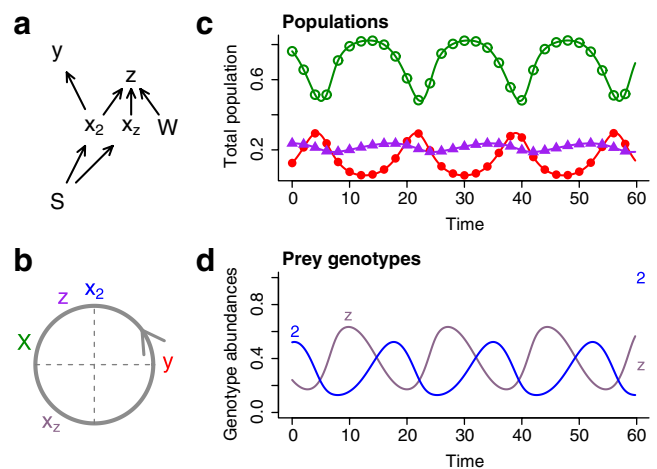


Fig. 10 LFC model dynamics when the ESC consists of the two prey types without defense against the intermediate predator z . For this figure, parameter values are such that the intermediate predator does not graze heavily on the focal prey x ($M = 1, \phi = 1, h = 0.25$)

quarter period or less, depending on how much it feeds on W versus x .

The IC model behaves the same way when h and η are small, so the $x \rightarrow z \rightarrow y$ chain is weak (Fig. 16 in the [Electronic supplementary material](#)). However, it can behave very differently when h and η are large (Fig. 11). Each predator becomes synchronized with one of the prey types (y with x_2 and z with x_z), while the prey remain out of phase with each other. This is similar to what occurs when the ESC consists of the two defended types (Figs. 8 and 14), except that one of the predators' peaks are synchronized with the peaks in total prey abundance, rather than with the troughs in total prey abundance.

Free for all The final possibility is the three-genotype ESC of x_2, x_y and x_z (diagrammed in Fig. 17a in the [Electronic supplementary material](#)). The analytic expressions for phase lags are much more complicated in this case than those for the two-genotype ESCs, so our study of this scenario is entirely numerical.

One generality is that the two types that y can eat, x_2 and x_y , tend to synchronize because the $y \leftrightarrow x$ interaction is the dominant link that drives the cycles; Fig. 17 in the [Electronic supplementary material](#) shows an example. But the three-type ESC still has enough “degrees of freedom” to behave in a variety of ways. For example, the three-type ESC will behave like the x_y, x_z ESC when x_z is rare and like the x_2, x_z ESC when x_y is rare, so the behaviors in Figs. 8, 9, 10, 11, 14 and 16 are all possible.

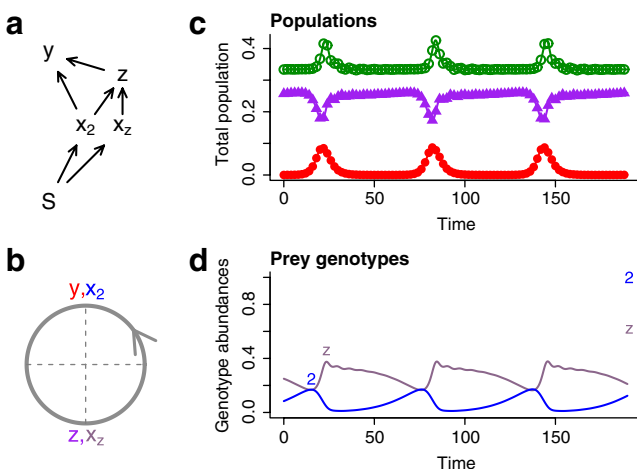


Fig. 11 IC model dynamics when the ESC consists of the two prey types without defense against the intermediate predator z , and the $x \rightarrow z \rightarrow y$ chain is not weak ($h = 3, \eta = 2$). Total prey X is not shown in (b) because its phase could not be uniquely determined by our analytic approximations

However, the main effect of the added state variable is that large-amplitude oscillations are typically chaotic rather than periodic. Phase relations vary over time (e.g., Fig. 12a), so reaching conclusions about the underlying food web structure based on patterns in population-level phase relations is much harder (though not always impossible—see Benincà et al. 2009). This same difficulty arises any time population dynamics are aperiodic.

Evidence for prey evolution therefore must be sought in different features of the food web dynamics. To do so, we combine ideas from Shertzer et al. (2002) and Hooker (2009). Using models and experimental data, Shertzer et al. (2002) showed that prey evolution in a one-predator food chain was revealed by a non-unique relationship between prey abundance and predator instantaneous growth rate. The observation that the same prey abundance was at some times sufficient for predator population growth, and at other times insufficient, was interpreted as evidence that prey quality was changing over time. We observe the same pattern in the multispecies food web, Fig. 12b, c, where we plot $\frac{1}{y} \frac{dy}{dt}$ and $\frac{1}{z} \frac{dz}{dt}$ as functions of the total abundance of the focal prey, X . However, the conclusion that prey quality must be changing depends on ruling out other possible causes for variation in predator population growth. In a multispecies food web that cannot be done, because the predators' per capita growth rates do not just depend on the abundance and edibility of a single prey species.

Instead, we need to estimate the contribution of possibly changing food quality to variation in predator population growth rates, as an addition to the other factors known to be present. Inspired by Hooker (2009), we formulated this problem as estimation of a smoothly time-varying perturbation to a dynamic model in which predator population growth rates depend on the total abundances of the species in the food web. We assumed that the functional responses and food web structure are known, but not the parameter values. That is, for the IC model we assumed

$$\begin{aligned} \frac{1}{y} \frac{dy}{dt} &= \frac{G\bar{p}(t)X(t)}{K + \bar{p}(t)X(t)} + ez - d \\ \frac{1}{z} \frac{dz}{dt} &= H\bar{\pi}(t)X(t) - Ey - D. \end{aligned} \quad (4)$$

The interpretation of (4) for this analysis is that the population totals $y(t)$, $z(t)$ and $X(t)$ are observed, but the parameters G, K, e, d, H, E, D and the time-varying mean food qualities $\bar{p}(t)$, $\bar{\pi}(t)$ all need to be

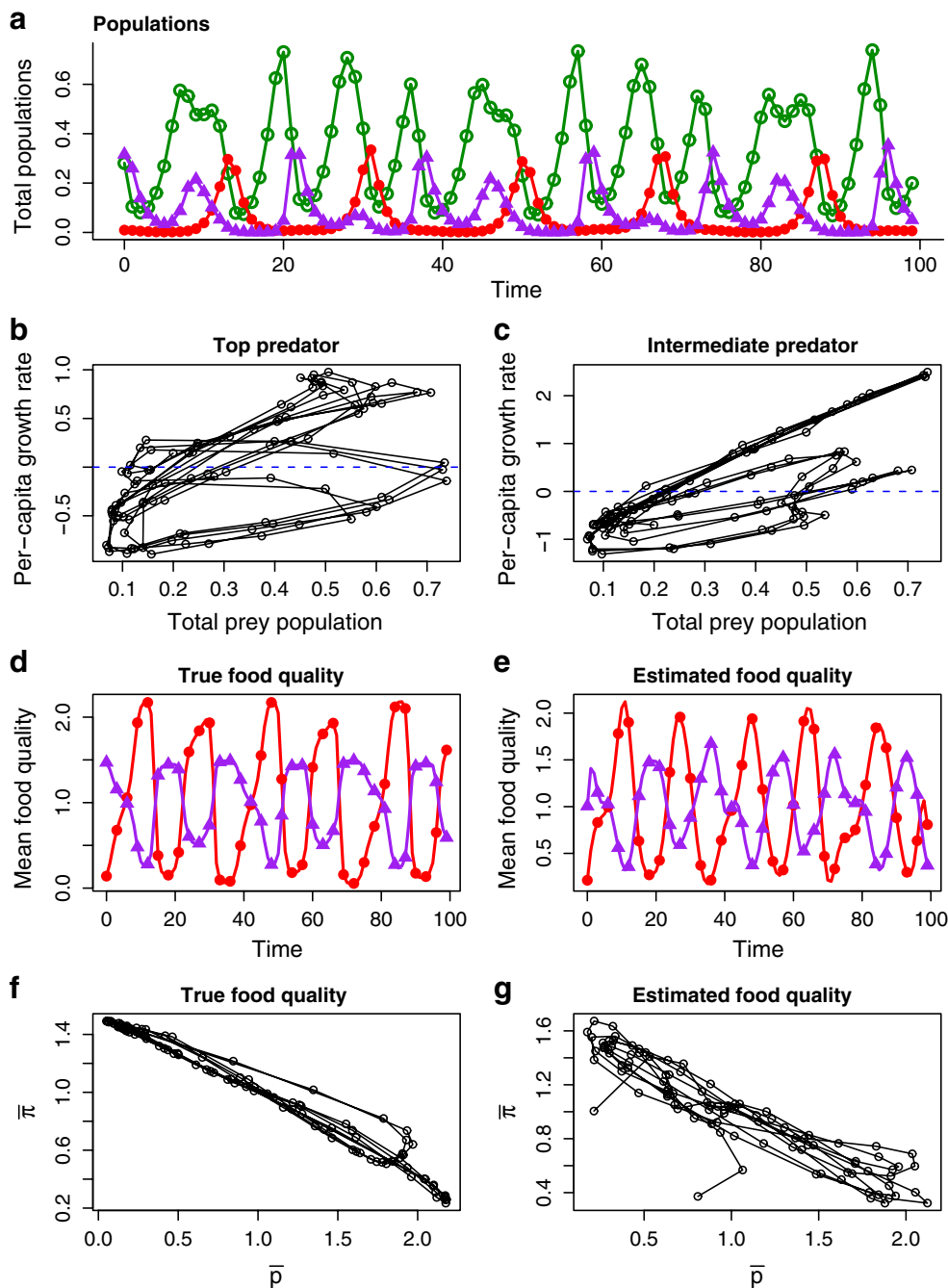


Fig. 12 Chaotic dynamics in the IC model when the ESC includes all three prey types that are vulnerable to attack by one or both predators. Symbols and colors are the same as in Fig. 1. **a** The population dynamics “data” (100 values of each population) that will be analyzed for evidence of prey evolution. Plots covering a longer time period confirm that the dynamics are either chaos or a very long chaotic transient. **b, c** Relationship between total abundance of the focal prey x , and per-capita population growth rates of the top and intermediate predators. Growth rates were estimated by spline-interpolating log-transformed population totals and

computing the derivative of the spline. **d, e** True and estimated dynamics of prey mean qualities $\bar{p}(t)$ (red, circles) and $\bar{\pi}(t)$ (purple, triangles); symbols and colors are the same as those used for the corresponding predator in panel (a). (**f, g**) True and estimated relationships between $\bar{p}(t)$ and $\bar{\pi}(t)$. In (**d–g**) $\bar{p}(t)$ and $\bar{\pi}(t)$ are both scaled relative to their mean values for plotting; note that because of the way the models are specified in Eq. 4, absolute food quality and maximum grazing rate are confounded, so only relative changes in food quality can be estimated

estimated. We used a *gradient matching* approach (Ellner et al. 2002), meaning that we began by estimating the left-hand sides of (4) by fitting a smooth curve to the observed y and z values. Fitting the right-hand sides of (4) to the estimated left-hand sides is then a non-linear regression problem. Gradient matching methods have been proposed numerous times in applications (e.g. Bellman and Roth 1971; Swartz and Bremermann 1975; Varah 1982; Ellner et al. 1997) and recently their statistical properties have been studied (Brunel 2008), proving that consistent parameter estimates can be obtained.

The functions $\bar{p}(t)$ and $\bar{\pi}(t)$ were modeled using basis expansion methods,

$$\bar{p}(t) = \sum_{j=1}^B c_j \varphi_j(t) \quad (5)$$

and similarly for $\bar{\pi}(t)$, where the functions $\varphi_j(t)$ are the cubic B-spline basis with evenly spaced knots on the time period of data collection (the “data” in this case being the 100 population values for X, y , and z plotted in Fig. 12a). The number of basis functions B was chosen by a simple cross-validation method: fitting to 75 randomly chosen values of predator population growth rate, and evaluating the out-of-sample forecasting accuracy on the remaining 25 data points, for M ranging from 10 to 40 in increments of 5. For both y and z , this gave $B = 30$ as the best complexity for estimating food quality dynamics.

The results (Fig. 12) indicate that the dynamics of food quality, as perceived by the two predators, can be recovered successfully from the predator and prey population dynamics. The main patterns are recovered correctly, in particular the fact that \bar{p} and $\bar{\pi}$ are almost perfectly out-of-phase (though not exactly out of phase, as they would be necessarily if only two genotypes were present). Also, because AIC is asymptotically equivalent to a comparison of out-of-sample likelihood values (Konishi and Kitagawa 2008), the data-driven choice of model complexity can be interpreted as showing that a model with time-varying food quality for both y and z would be selected (correctly) based on AIC, over a model with constant food quality.

Proper development and testing of this approach is beyond our scope here - for example, to deal with measurement error in population counts, and to test for statistical significance of the inferred time-varying perturbations, by extending the analysis in Hooker (2009). The point of our exploratory exercise was to demonstrate that even when complex food web structure is accompanied by complex population dynamics, the

effects of rapid prey evolution will still be evident, and they can be detected by analyzing patterns of change in population growth rates.

Discussion

The results in this paper are a step towards understanding the potential role of rapid evolution in the dynamics of real food webs. Stepping back from the details, what we have learned is that greater food web complexity does not mask the effects of rapid prey evolution. Rather, we see the opposite: with the addition of more species to the web, there are new distinctive patterns that only become possible when prey evolve. The key requirement for these new types of dynamics to occur, within the scope of our models, is a strong tradeoff between two prey defense traits, each conferring defense against one of the two predators. The dynamics of food availability (quality times abundance) are then different for the two predators. This difference is what gives rise to the new patterns. If a single trait is effective against both predators, the two predators are instead synchronized by their common response to the prey, and the prey are synchronized by their common response to predation pressure, so the dynamics are like a one-predator food chain.

Information about the strengths of interactions between species is crucial for our understanding of how food webs function and persist (Berlow et al. 2004; Wootton and Emmerson 2005). Our results pose two challenges for one important approach for estimating interaction strengths, the analysis of multispecies time series data (e.g., Ives et al. 1999, 2003; Hampton et al. 2006). Statistical relationships between the abundance of one species, and the growth rate of another, are the basis in this approach for inferring the existence and strength of a trophic link. The first challenge is that dynamic changes in prey quality could easily obscure the strength of a genuine link. A common outcome in our models is that half of the peaks in the abundance of the focal prey are not followed by any response at all from the top predator. Analyses “blind” to prey evolution would at least underestimate the strength of the link, and might well conclude that there is no link whatsoever. In Fig. 12b there are even periods when the relationship between total prey abundance and top predator growth rate is negative. The second, more interesting challenge, is for researchers to revisit multispecies time series and examine whether patterns indicative of rapid evolution can now be identified, as Duffy et al. (2009) have recently done for an aquatic host-pathogen interaction.

Some other directions for future work are suggested by our findings.

The first is to go beyond strictly cyclic dynamics driven by consumer–resource interactions. Many populations are cyclic (Kendall et al. 1998). But the majority are not, so it is important to ask how other kinds of food web dynamics might be affected by rapid evolution. Dynamics driven by seasonality can also be influenced strongly by rapid trait dynamics in short-lived organisms (e.g., Ellner et al. 1999; Duffy and Sivars-Becker 2007; Duffy et al. 2008, 2009; Duffy and Hall 2008). On a longer time scale, populations are strongly affected by environmental variability on multiple time scales, ranging from uncorrelated interannual variability to decadal or longer large-scale climate oscillations (ENSO, NAO, PDO, etc.). In these situations, the dynamical possibilities without evolution are much broader, so distinctive patterns due to rapid evolution may be harder to detect. When prey defenses are predator-specific, prey evolution is revealed by the fact that two predators “see” the same prey population in different ways at the same time. Our brief examination of chaotic dynamics in the three-prey-clone system (Fig. 12) suggests that the dynamics of population growth rates (in relation to population sizes) holds the information needed to identify the presence of trait evolution, and to estimate the size of its impacts.

Secondly, the effects of rapid evolution should be studied in food webs of truly realistic complexity. Specifically, the longstanding question of how species-rich food webs with many trophic links can be stable should be re-examined in models where the traits determining the presence and strength of trophic links can evolve rapidly in response to changes in the abundances of potential prey and predators. Previous work has shown that trait dynamics can greatly promote stability in a predator–prey food chain (Abrams and Matsuda 1997; Cortez and Ellner 2010; Tien 2010). This is especially true when the cost of prey defense is state-dependent, so that avoidance of predation entails a higher reduction of population growth rate when resources are scarce than when resources are abundant (Tien 2010). However, prey evolution can also be destabilizing, in fact the combination of trait dynamics that converge to a stable equilibrium if population densities are held constant, and population dynamics that converge to a stable equilibrium if traits are held constant, can produce eco-evolutionary limit cycles around a locally unstable equilibrium (Cortez and Ellner 2010).

Eco-evolutionary models with realistic numbers of species and links will probably have to be studied computationally. Using such an approach, Kondoh (2007) showed that dynamic adjustment of defense effort by

prey species, in food webs of ten or fewer species with a range of structures, increased the probability of dynamic stability and could change the complexity–stability relationship. His equations for trait dynamics are more appropriate for inducible defenses or behavioral adjustments to predation risk (such as changing the amount of time spent foraging in different habitats), but we would expect similar effects from trait evolution models. Kondoh (2007) also found, as we did here, that the outcome depended on whether defense traits were predator-specific or universally effective. A related issue is how predictions change if the tradeoff curves favor intermediate types, rather than extremes as we have assumed. In that case the genetic variation would be expected to consist of a “cloud” of intermediate genotypes moving in response to selection, so the quantitative trait models described in Appendix A would be more appropriate than our clonal models. Intermediate trait values tend to stabilize the model, because the predator–prey link is weakened. But the close correspondence between clonal and quantitative trait models (Appendix A) suggests that their behaviors will be similar when cycles occur, implying that assumptions about the tradeoff between different defense traits are not very important for our predictions about population dynamics. Online Fig. 15 shows one example, but a full exploration of this issue is beyond our scope here.

Finally, rapid host evolution in host–pathogen interactions needs more study. The importance of pathogen evolution is widely recognized, for example the large literatures on evolution of virulence and evolution of drug resistance. This focus on pathogen evolution is not misguided. Generally the pathogen is much shorter-lived than the host, and resistance evolution has enormous practical importance. But disease-related mortality simultaneously decreases host lifespan and imposes strong selection, creating the opportunity and driving force for rapid host evolution. Empirical examples of rapid host evolution caused by disease (Dube et al. 2002; Duffy and Sivars-Becker 2007; Duncan and Little 2007; Zbinden et al. 2008) and its effects on the dynamics of infectious disease outbreaks (Duffy et al. 2009) have started to accrue. Challenges here, as with non-cyclic food web dynamics, will be to predict how rapid evolution affects the course of transient dynamics (a disease outbreak), and then to develop methods for detecting these effects in empirical data.

Acknowledgements We thank the Cornell EEB chemostat group (Aldo Barreiro Felpeto, Michael Cortez, Nelson G. Hairston Jr., Teppo Hiltunen, Giles Hooker, Laura E. Jones, Joseph Simonis, Yuefeng Wu) and two perceptive anonymous referees for their advice and comments on the manuscript.

Appendix

A Trait dynamics in clonal versus sexually reproducing prey

Here, we show that many of our results are also relevant to sexually reproducing prey because our clonal evolution model can be re-expressed as a gradient dynamics model for trait evolution in a sexual species.

Let x_1 and x_2 be the abundances of the two prey clones, $X = x_1 + x_2$, and let $f = x_2/(x_1 + x_2)$. We need to re-write the model in terms of X , the total prey population, and its “trait mean” f , rather than x_1 and x_2 . In the predator and substrate equations, we just substitute $x_2 = fX$, $x_1 = (1 - f)X$, so that for example $Q = ((1 - f)p_1 + fp_2)X$. The dynamic equation for f is (omitting some algebra)

$$\begin{aligned} \dot{f} &= \frac{d}{dt} \left(\frac{x_2}{x_1 + x_2} \right) = f(1 - f) \left[\frac{\dot{x}_2}{x_2} - \frac{\dot{x}_1}{x_1} \right] \\ &= f(1 - f)(W_2 - W_1) \end{aligned} \tag{6}$$

where W_i is the fitness of prey type i . Note that f is the population mean of the trait whose value is 1 for clone-2 individuals, and 0 for clone-1 individuals, and $f(1 - f)$ is the population variance for this trait. The dynamic equation for X is

$$\dot{X} = \dot{x}_1 + \dot{x}_2 = x_1 W_1 + x_2 W_2 = X [(1 - f)W_1 + fW_2]. \tag{7}$$

Comparing the last two equations, we see that the rate of change in f is the trait variance $f(1 - f)$ multiplying the gradient with respect to f of prey fitness \dot{X}/X with the predator’s grazing rate $g/(k_y + Q)$ held constant, which is the fitness gradient for a rare invader. Thus, our two-clone model is equivalent to a gradient-dynamics model for frequency-dependent evolution of the defense trait in a sexually reproducing species. Inherited from this model’s asexual origins are the form of the mean-variance relationship, and the relationship between mean trait value f and per-capita nutrient uptake rate in the quantitative trait model, namely $\frac{(1-f)m_1S}{k_1+S} + \frac{fm_2S}{k_2+S}$. But mean-variance relationships like the one in (6) have often been assumed to model traits limited to a finite interval (such as fractional allocations), and while the nutrient uptake rate is not a standard model, it’s not any less reasonable than specifying m and k directly as a function of the mean defense level.

With three or more clones the correspondence between clonal and sexual models is no longer exact. Let f_i denote the population mean of the trait which

has value 1 for clone i , for all other clones (i.e., the frequency of clone i). Then calculations similar to those above show that $\dot{f}_i = f_i(1 - f_i) \frac{\partial \dot{X}}{\partial f_i X}$, if the derivative with respect to f_i is taken by increasing f_i and decreasing all other clone frequencies by a constant fraction of their value while maintaining $\sum_j f_j = 1$ and holding

the predator grazing rate constant. So we get gradient dynamics, but not a standard model for correlated quantitative traits in a sexual species. It remains an open question whether the complex dynamics seen in our model with three clones would also be seen in a model for sexually reproducing prey.

B Calculating phase lags

Here we explain our method for computing approximate phase lags, which we implemented using computer algebra. The oscillations in our model appear to always arise through a supercritical Hopf bifurcation, as in the one-predator model. We compute approximate phase lags for parameters just past that bifurcation. Solutions $\mathbf{x}(t)$ are then small-amplitude oscillations about an equilibrium with common period T , and $x_j(t)$ is approximately proportional to $\sin(\lambda t + \psi_j)$ where $\lambda = 2\pi/T$ and ψ_j is the phase for component j .

To compute relative phases, we choose one solution component (say x_0) as the reference and set the origin of time so that $\psi_0 = 0$. The other components (which we still denote $\mathbf{x}(t)$) then satisfy a forced nonlinear system $\dot{\mathbf{x}} = \mathbf{F}(\mathbf{x}, x_0(t))$ where $x_0(t) = \varepsilon \sin(\lambda t)$ is regarded as an exogenous forcing term. The linearized system for deviations from equilibrium can be written as

$$\dot{\mathbf{x}} = \mathbf{J}\mathbf{x} + \mathbf{u}(t) \tag{8}$$

where \mathbf{J} is the Jacobian matrix of \mathbf{F} at the equilibrium, $\mathbf{x}(t)$ is now the m -vector of deviations from the equilibrium, and $\mathbf{u}(t) = \varepsilon \sin(\lambda t) \frac{\partial \mathbf{F}}{\partial x_0}$ is the forcing. The asymptotic solutions to (8) are

$$\begin{aligned} x_i(t) &= A_i \cos(\lambda t) + B_i \sin(\lambda t), \\ \text{with } u_i(t) &= b_i \sin(\lambda t), \quad b_i = \varepsilon \frac{\partial \mathbf{F}_i}{\partial x_0}. \end{aligned} \tag{9}$$

The unknown A ’s and B ’s, which determine the phase lags, can be found by writing (8) as a matrix equation. Differentiation of \mathbf{x} is accomplished by transforming $A_i \rightarrow \lambda B_i$, $B_i \rightarrow -\lambda A_i$. Defining

$$\begin{aligned} \mathbf{X} &= (B_1, B_2, \dots, B_m, A_1, A_2, \dots, A_m) \\ \mathbf{U} &= (b_1, b_2, \dots, b_m, 0, 0, \dots, 0) \end{aligned} \tag{10}$$

differentiation of \mathbf{x} is represented by the matrix $\mathbf{D} = \begin{bmatrix} 0 & -\lambda \mathbf{I} \\ \lambda \mathbf{I} & 0 \end{bmatrix}$ and multiplication by \mathbf{J} by the matrix $\mathbf{J}_2 = \begin{bmatrix} \mathbf{J} & 0 \\ 0 & \mathbf{J} \end{bmatrix}$. The coefficient representation of (8) is therefore $\mathbf{D}\mathbf{X} = \mathbf{J}_2\mathbf{X} + \mathbf{U}$ with solution $\mathbf{X} = (\mathbf{D} - \mathbf{J}_2)^{-1}\mathbf{U}$. The blocks in $\mathbf{D} - \mathbf{J}_2$ commute, so defining $\mathbf{R} = (\mathbf{J}^2 + \lambda^2\mathbf{I})^{-1}$, we have

$$(\mathbf{D} - \mathbf{J}_2)^{-1} = \begin{bmatrix} -\mathbf{R}\mathbf{J} & \lambda\mathbf{R} \\ -\lambda\mathbf{R} & -\mathbf{R}\mathbf{J} \end{bmatrix}. \tag{11}$$

The addition formula $\sin(\lambda t + \psi) = \sin(\psi)\cos(\lambda t) + \cos(\psi)\sin(\lambda t)$ shows that the phase ψ_i of $x_i(t)$ relative to $\sin(\lambda t)$ has the properties

$$\begin{aligned} \sin(\psi_i) &= A_i/\rho, \text{ where } \rho = \sqrt{A_i^2 + B_i^2} \\ \cos(\psi_i) &= B_i/\rho \\ \tan(\psi_i) &= A_i/B_i. \end{aligned} \tag{12}$$

The value of ψ_i is therefore uniquely determined by the signs and ratio of A_i and B_i , so we can compute any convenient positive multiple of (A_i, B_i) . As a visual aid for readers, Fig. 18 in the [Electronic supplementary material](#) shows how the scaled coefficients (A_i, B_i) relate to phase differences with the forcing variable.

The main limit to this method is that the expressions for A and B become very complicated as the number of state variables goes up, because they are symbolic solutions of a high-dimensional, non-sparse linear system. For scenarios with one or two prey genotypes we can make sense of the expressions for phase lags, at least in ecologically relevant limits of the parameter values, but with three genotypes it exceeds our abilities and we have to study the system numerically.

C LFC model without prey evolution

Here we consider LFC model (2) when there is only one genotype in the focal prey species x , assuming that all state variables have small oscillations around their mean values. The top predator only feeds on x , so it lags x by a quarter period (Bulmer 1975). The intermediate predator can behave differently because it is driven by both x and W . Writing $x = \bar{x}(1 + \varepsilon \sin(\lambda t))$ where $\lambda = 2\pi/T$ and T is the cycle period, the relevant sub-system is

$$\begin{aligned} \dot{z} &= z(hx(t) + \phi w - 1) \\ \dot{w} &= M - w - \phi zw \end{aligned} \tag{13}$$

Without forcing (i.e. $\varepsilon = 0$), (13) has steady state

$$\bar{w} = \frac{1 - h\bar{x}}{\phi}, \bar{z} = \frac{M - \bar{w}}{\phi\bar{w}}. \tag{14}$$

This is a stable node whenever parameters are such that \bar{w} and \bar{z} are positive (the Jacobian has trace $-(1 + \phi\bar{z}) < 0$ and determinant $\phi^2\bar{z}\bar{w} > 0$), and numerical evidence suggests that it is globally stable (so far, no luck with the Bendixson–Dulac negative criterion). The forced system ($\varepsilon > 0$) is therefore “chasing” a moving equilibrium $(\bar{z}(t), \bar{w}(t))$ in which $\bar{z}(t)$ is a monotonically increasing function of $x(t)$, hence $z(t)$ exhibits oscillations that track $x(t)$ but lag behind it.

To be more precise, the phase lag for small oscillations can be calculated by the method in Appendix B for the system (13) linearized about the steady-state $(\bar{z}, \bar{w}, \bar{x})$ for $\varepsilon = 0$. These calculations yield that $z(t) - \bar{z}$ is proportional to $\sin(\lambda t + \psi)$ where $\sin(\psi) < 0$, $\cos(\psi) > 0$ and

$$\tan(\psi) = -\frac{\lambda^3 + ((\phi\bar{z} + 1)^2 - \phi^2\bar{w}\bar{z})\lambda}{\phi^2\bar{w}\bar{z}(\phi\bar{z} + 1)} \tag{15}$$

(note that because $\phi\bar{w} = 1 - h\bar{x} < 1$, the numerator on the right-hand side of (15) is positive, hence $\tan(\psi) < 0$). These properties imply that $\psi \in (-\pi/2, 0)$, so z lags behind x by an amount that approaches the upper limit of one quarter cycle period when $\tan(\psi)$ is very large in magnitude, and approaches zero (relative to T) when $\tan(\psi)$ is small.

Although the expression for $\tan(\psi)$ is complicated, some situations can be identified in which the lag is predicted to be short vs. long relative to T .

- Because $\lambda \rightarrow 0$ as $T \rightarrow \infty$, the ratio between the lag and the cycle period goes to zero as the cycle period increases. That is, when the cycle period is very long, the dynamics of z and W become “slaved” to $x(t)$, and $z(t)$ is almost exactly at the value of \bar{z} determined by the current value of $x(t)$.
- The right-hand side of (15) can be written as

$$-\frac{\lambda\Omega + \lambda^3(1 - h\bar{x})^2}{\phi M(1 - h\bar{x})(\phi M + h\bar{x} - 1)}. \tag{16}$$

where $\Omega > 0$ and all terms in the denominator of (16) are positive so long as $\bar{w}, \bar{z} > 0$. The lag therefore approaches the quarter-period limit when the denominator goes to 0. One way that this happens is when $h\bar{x} \rightarrow 1$, meaning that the intermediate predator is grazing heavily on the focal prey species

and reaching high enough densities that its alternate food W is driven to very low levels ($\bar{w} \rightarrow 0$). The intermediate predator is then almost a specialist on the focal prey species, so it has the classical quarter-period lag behind the focal prey.

- The other way for the denominator of (16) to go to zero is if ϕ decreases to $(1 - h\bar{x})/M$. This is the value of ϕ at which $\bar{z} = 0$ when $x = \bar{x}$. The intermediate predator therefore increases only when the focal prey species is more abundant (above \bar{x}), and is heading for extinction whenever the focal prey species is less abundant. The intermediate predator therefore behaves as if the focal prey were its main food source, even if $h\bar{x}$ is small.

Numerical evaluations of (15) indicate that the effects of h and ϕ hold generally: any increase in h or decrease in ϕ causes the linearized system’s phase lag to increase. The accuracy of (16) for the nonlinear system (13) is very good for small fluctuations (Fig. 19a in the [Electronic supplementary material](#)) and remains fairly good for substantial fluctuations (19b, in which the cycle peak is roughly three times the trough). The linearized analysis generally under-predicts the lag by a bit, and is most accurate near the extremes of zero or quarter-period lag.

D IC model without prey evolution

As the second baseline case, we calculate here the approximate phase relations between x , y and z in the Intermediate Consumer model with only one prey type. It is simplest to take $x(t)$ as the forcing function and determine the phase lags of y and z relative to x . The equations for this scenario are

$$\begin{aligned} \dot{y} &= y \left[\frac{gx(t)}{k_y + x(t)} + \eta z - 1 \right] \\ \dot{z} &= z [hx(t) - \eta y - 1] \end{aligned} \tag{17}$$

As before we set $x(t) = \bar{x}(1 + \varepsilon \sin(\lambda t))$, and assume small oscillations of y and z about \bar{y} and \bar{z} , the equilibria of (17) when $x(t) \equiv \bar{x}$,

$$\begin{aligned} \bar{z} &= (1 - G\bar{x})/\eta, \quad \bar{y} = (h\bar{x} - 1)/\eta \\ \text{where } G &= g/(k_y + \bar{x}). \end{aligned} \tag{18}$$

We must have $G\bar{x} < 1$, $h\bar{x} > 1$ for the equilibrium to exist. These inequalities correspond to z being the more effective predator, able to persist on x alone, while y depends on consuming z as well as x in order to persist.

The method of Appendix B can be applied to the linearization of (17). Note that these calculations are relevant to the full three-variable food web model at parameter values that generate a small-amplitude limit cycle, rather than to the dynamics of (17) on its own without any feedbacks from y and z to x . The results (up to a positive factor) are

$$\begin{aligned} A_y &= -gk_y\lambda, & B_y &= -h(\bar{x} + k_y)^2\eta\bar{z} \\ A_z &= -h(\bar{x} + k_y)^2\lambda, & B_z &= gk_y\bar{y}. \end{aligned} \tag{19}$$

The signs of the A ’s and B ’s imply that $\psi_y \in (-\pi, -\pi/2)$, meaning a lag between quarter and half the cycle period, while $\psi_z \in (-\pi/2, 0)$, a phase lag of under a quarter period. These are exactly what the food web structure suggests: because y and z both feed on x and therefore should lag x by a quarter period, but at the same time y feeds on z so it should lag z by a quarter period. The outcome is a compromise between these two expectations determined by the relative importance of the direct and indirect paths between x and y . In particular, when either predator becomes rare, the other converges to a quarter period lag behind x ($B = \cos(\psi) \rightarrow 0$).

The “positive factor” in the previous paragraph requires some comment. Dividing out some strictly positive factors (such as $\bar{x} + k_y$) it is

$$D = (\bar{x} + k_y)\lambda^2 + (g - 1)h\bar{x}^2 + (1 - hk_y - g)\bar{x} + k_y. \tag{20}$$

The sign of D is not obvious, and it depends on the cycle period T . Setting $\lambda = 0$ in D , the result is a negative multiple of \bar{z} . To determine the actual sign of D we therefore must estimate the cycle period of the full food chain. This was done by determining the period at the point where limit cycles arise through a Hopf bifurcation, for two cases. The first is the S, x, y system with z absent. This system reduces to two dimensions because asymptotically $S + x + y \equiv 1$. At the Hopf bifurcation point the eigenvalues of the Jacobian \mathbf{J} are $\pm i\lambda$, so $\lambda^2 = \det(\mathbf{J})$. Substituting the resulting value of λ^2 into D , gives $D = \lambda^2 g k_y / (g - 1)$ which is positive because $g > 1$ must hold for the predator to persist. The second case is the complete x, y, z food web but with exponential growth of the prey (i.e., S is absent, and $\dot{x} = rx -$ predation). In that case λ^2 at the Hopf bifurcation equals the product of all Jacobian eigenvalues divided by their sum, which is c_2/c_0 where c_k is the k^{th} order coefficient in the characteristic polynomial of \mathbf{J} . The resulting value of (20) is the product of strictly positive terms and some of the c_j , which by the Routh–Hurwitz criterion

are all positive at the Hopf bifurcation point, hence D is positive. Code for these calculations in MAXIMA (maxima.sourceforge.net) is available on request from SPE. The full S, x, y, z model has not yet succumbed to this approach, but numerical evidence supports the belief that D is positive whenever the system has a limit cycle.

E Two prey genotypes

In this Appendix we consider scenarios in which the ESC consists of two prey genotypes. In order for eco-evolutionary cycles to occur, one genotype must be defended against top predator y while the other is vulnerable to predation by y . For simplicity we assume that defense is 100% effective, though numerical solutions of the model assume that defense is imperfect. Also, we assume that $\lambda \ll 1$ because eco-evolutionary cycles typically have a long period (Jones and Ellner 2007), and usually discard terms of $O(\lambda^2)$ or higher in calculations.

E.1 One predator

The starting point is a system with only the top predator y , the scenario leading to “evolutionary cycles” in our previous studies. In the limit of vanishingly small cost for defense, we have shown (Jones and Ellner 2007) that the two prey genotypes oscillate almost exactly out of phase, while y (lagging the edible prey type by a quarter period) is out of phase with total prey abundance. However numerical solutions of the model (e.g., Yoshida et al. 2003) show the same pattern even when the defense cost is substantial. Here we confirm the numerical results, as a general approximation when the cycle period is long and prey population growth rate is sensitive to changes in limiting substrate concentration.

The persisting prey genotypes are x_0 and x_2 (Fig. 2). Because y feeds only on x_2 , it will lag x_2 by a quarter period. To determine the other lags we can therefore regard S and x_0 as forced by the oscillations in x_2 . The equations for that subsystem are

$$\begin{aligned} \dot{S} &= 1 - S - \frac{mS(x_2(t) + x_0)}{k_c + S} \\ \dot{x}_0 &= x_0 \left[\frac{mS}{k_c + S} - 1 \right] \end{aligned} \tag{21}$$

with $x_2(t) = \bar{x}_2(1 + \varepsilon \sin(\lambda t))$.

The only nonlinear term is x_0 's functional response $f(S) = mS/(k_c + S)$, which produces in entries contain-

ing $f'(\bar{S})$ in the first column of the Jacobian for (21). Defining $b = f'(\bar{S})$ the Jacobian is

$$\begin{aligned} \mathbf{J} &= \begin{bmatrix} -1 - b(\bar{x}_2 + \bar{x}_0) - \frac{m\bar{S}}{k_c + \bar{S}} & \\ b\bar{x}_0 & 0 \end{bmatrix} \\ &= \begin{bmatrix} -1 - b(\bar{x}_2 + \bar{x}_0) - 1 & \\ b\bar{x}_0 & 0 \end{bmatrix}. \end{aligned}$$

In the notation of Appendix B, the forcing coefficient vector \mathbf{U} is proportional to $(-1, 0)$. The procedure in Appendix B produces for x_0 (up to a positive rescaling that depends on the forcing amplitude)

$$A = \lambda(b^{-1} + \bar{x}_2 + \bar{x}_0), \quad B = \lambda^2 b^{-1} - \bar{x}_0. \tag{22}$$

In this paper typically $\lambda \ll 1$ because the cycles are long-period cycles driven by evolution, and b will be large because prey are potentially rapid-growing but limited by nutrient scarcity at equilibrium. Then to leading order (22) becomes $A = \lambda(\bar{x}_2 + \bar{x}_0)$, $B = -\bar{x}_0$. This implies that to leading order in λ , the phase of x_0 relative to x_2 is $\psi = \arctan(A/B) = -\pi - \lambda(1 + \bar{x}_2/\bar{x}_0)$. Therefore

$$\begin{aligned} \sin(\lambda t + \psi) &\approx \sin(\lambda t - \pi - \lambda(1 + \bar{x}_2/\bar{x}_0)) \\ &= \sin(\lambda(t - 1 - \bar{x}_2/\bar{x}_0) - \pi). \end{aligned} \tag{23}$$

The defended prey type therefore lags the edible prey type by slightly more than half a cycle period, with the lag exceeding half the period by at least one unit of scaled time (which in dimensional time units is the inverse of the dilution rate). The defended prey type is only linked to S , so it lags S by a quarter period, hence S must lag the edible prey by a quarter period plus (to leading order) $1 + \bar{x}_2/\bar{x}_0$ time units.

Figure 2 shows a numerical example, and as predicted the defended prey lags the edible prey by slightly more than half the cycle period. This small asymmetry has the important consequence that the peak in total prey abundance occurs in between a peak in defended prey and the subsequent peak in edible prey, and roughly halfway in between. Peaks therefore occur in the sequence

defended type \rightarrow total prey \rightarrow edible type \rightarrow predator

with roughly a quarter-period lag between each. The slight deviation of the prey types from being perfectly out of phase is thus the underlying cause for the half-period lag between predator and total prey abundance, which is the defining feature of “evolutionary cycles” in the one-predator food chain.

E.2 Two predators

Now we add back the second predator z , still assuming that there are two prey genotypes, one highly vulnerable to y and the other well defended against y .

Firstly, suppose the defense against y is also effective against z , so the persisting prey clones are x_2 and x_0 . Then (as discussed in the main text) the (x_2, y, z) system is equivalent to the two-predator systems with uniform non-evolving prey x considered in Appendices C and D, and the results from those Appendices apply. x_0 is linked to the (x_2, y, z) system only through the substrate, so the results in Appendix E.1 apply, meaning that x_0 will lag x_2 by slightly more than half the cycle period. Figure 13 illustrates these for the IC model; for the LFC model see Fig. 7 in the main text.

Secondly, suppose that defenses against y and against z are incompatible, so the persisting prey clones are x_y and x_z . Then in the linked food chains model, the (y, x_y) and the (z, x_z) subsystems are both equivalent to a system of one predator feeding on a non-evolving prey type, so y lags x_y by a quarter period, and z lags x_z by a quarter period or less depending on how much it feeds on W . To determine the lag between the prey types we can take x_y as the forcing variable and consider the subsystem

$$\begin{aligned} \dot{S} &= 1 - S - x_z f_z(S) - x_y(t) f_y(S) \\ \dot{x}_z &= x_z [f_z(S) - hz - 1] \\ \dot{z} &= z [hx_z + \phi W - 1] \\ \dot{W} &= M - W - \phi z W \end{aligned} \tag{24}$$

where f_y, f_z are the algal types' functional responses. Applying Appendix B gives that the prey types are roughly out of phase: as $\lambda \rightarrow 0$ we have $A \rightarrow 0, B < 0$ for the phase lag of x_z relative to x_y , which implies a half-period lag. The $O(\lambda)$ term in A is a complicated expression whose sign cannot be determined in general, but it is negative when z 's second food source is relatively unimportant ($\phi \bar{w} \ll 1$) implying that the lag is slightly under a half period.

In the IC model, again considering the other variables as forced by x_y , the equations are

$$\begin{aligned} \dot{S} &= 1 - S - x_z f_z(S) - x_y(t) f_y(S) \\ \dot{x}_z &= x_z [f_z(S) - hz - 1] \\ \dot{z} &= z [hx_z - \eta y - 1] \\ \dot{y} &= y \left[\frac{gx_y(t)}{k_y + x_y(t)} + \eta z - 1 \right] \end{aligned} \tag{25}$$

Applying Appendix B, we obtain the following results for $\lambda \ll 1$. In the limit $h = \eta = 0$ the food web (25) is equivalent to the one-predator evolutionary cycles scenario, so x_z lags x_y by a half period plus an amount of $O(\lambda)$. With h and η increasing from 0 in constant proportion ($\eta = dh$), the derivative of $\tan(\psi)$ is $O(\lambda) > 0$, indicating a decrease in lag, and $\tan(\psi) = O(\lambda/h) < 0$ as $h \rightarrow \infty$, so the lag converges to exactly a half period. The $h \rightarrow \infty$ limit is not actually relevant, because the $x_y \rightarrow y$ link has to be dominant for cycles to occur, but the limit indicates the direction of change as the $x_z \rightarrow z \rightarrow y$ pathway increases in importance. y lags x_y by a quarter period for $h = \eta = 0$ ($A = 0(1) < 0, B = O(\lambda)$), and the lag increases to a half period as $h \rightarrow \infty$ with η increasing in proportion ($A = O(\lambda/h) > 0, B = O(1) < 0$). z is only linked to x_z when $\eta = 0$, so it then lags x_z by a quarter period. As the $x_z \rightarrow z \rightarrow y$ path is strengthened, the linearized analysis predicts an increase in lag to a half period within $O(\lambda)$, meaning that z 's lag behind x_z shrinks.

Figure 14 illustrates these predictions, for $\eta = 0.5, h = 4$ meaning that the $z \leftrightarrow y$ link is weaker than the $z \leftrightarrow x$ link, but not vanishingly small. As predicted by the linear analysis, peaks in y lag peaks in x_y by slightly more than a quarter period (30%), while peaks in z lag peaks in x_z by slightly less (18%).

The final scenario with two prey types is coexistence of x_z and x_2 , the types with no defense against z (Fig. 10). For the LFC model, with x_2 as the forcing function the equations for the forced variables are

$$\begin{aligned} \dot{S} &= 1 - S - x_z f_z(S) - x_2(t) f_2(S) \\ \dot{x}_z &= x_z [f_z(S) - hz - 1] \\ \dot{y} &= y \left[\frac{gx_2(t)}{k_y + x_2(t)} - 1 \right] \\ \dot{z} &= z [h(x_z + x_2(t)) + \phi W - 1] \\ \dot{W} &= M - W - \phi z W \end{aligned} \tag{26}$$

where $f_i(S)$ are the prey functional responses. The method in Appendix B yields that the lag of x_z relative to x_2 when $\lambda \ll 1$ is a half-period plus an amount of order λ (specifically, $\tan(\psi) = A/B = O(\lambda)$ with $A = O(\lambda) > 0, B = O(1) < 0$ for λ small). Everything else follows from the food web structure and previous results, as described in the main text.

For the IC model, the equations for the forced variables are the first two lines of (26) plus

$$\begin{aligned} \dot{y} &= y \left[\frac{gx_2(t)}{k_y + x_2(t)} + \eta z - 1 \right] \\ \dot{z} &= z [h(x_z + x_2(t)) - \eta y - 1] \end{aligned} \tag{27}$$

For $h, \eta \rightarrow 0$ the (y, x_2, x_z) subsystem reduces to one-predator evolutionary cycles, so x_z and x_2 are nearly out of phase, y is out of phase with total prey and z lags total prey by a quarter period. When the intermediate predator becomes important (increasing h and η in constant proportion), x_z and x_2 remain out of phase ($A = O(\lambda/h) > 0, B = O(1) < 0$), but the predator lags are completely different: y becomes synchronized with x_2 ($A = O(\lambda) > 0, B = O(1) > 0$), while z is out of phase with x_2 ($A = O(\lambda/h) > 0, B = O(1) < 0$), and therefore synchronized within $O(\lambda)$ with x_z . The result is that the two predators are out of phase with each other (Fig. 11). Because the two prey types become almost exactly synchronous, two things occur: the cycles of total prey abundance become “cryptic” (Yoshida et al. 2007), and peaks in total prey coincide with peaks in one of the two prey types (at some time when $\dot{x}_z = \dot{x}_2 = 0$). As a result, one predator is in phase with total prey abundance, and the other is out of phase with total prey abundance.

References

- Abrams PA (2000) The evolution of predator–prey interactions: theory and evidence. *Ann Rev Ecol Syst* 31:79–105
- Abrams PA, Matsuda H (1997) Prey adaptation as a cause of predator–prey cycles. *Evolution* 51:1742–1750
- Becks L, Hilker FM, Malchow H, Jurgens K, Arndt H (2005) Experimental demonstration of chaos in a microbial food web. *Nature* 435:1226–1229
- Becks L, Ellner SP, Jones LE, Hairston NG Jr (2010) Reduction of adaptive genetic diversity radically alters eco-evolutionary community dynamics. *Ecol Lett* 13(8):989–997
- Bellman R, Roth RS (1971) The use of splines with unknown end points in the identification of systems. *J Math Anal Appl* 34:26–33
- Benincà E, Huisman J, Heerkloss R, Jöhnk KD, Branco P, Van Nes EH, Scheffer M, Ellner SP (2008) Chaos in a long-term experiment with a plankton community. *Nature* 451:822–825
- Benincà E, Jöhnk KD, Heerkloss R, Huisman J (2009) Coupled predator–prey oscillations in a chaotic food web. *Ecol Lett* 12:1367–1378
- Berlow EL, Neutel AM, Cohen JE, Ruitter PCd, Ebenman B, Emmerson M, Fox JW, Jansen VAA, Jones JJ, Kokkoris GD, Logofet DO, McKane AJ, Montoya JM, Petchey O (2004) Interaction strengths in food webs: issues and opportunities. *J Anim Ecol* 73:585–598
- Brunel J-B (2008) Parameter estimation of ODE’s via nonparametric estimators. *Electron J Stat* 2:1242–1267
- Bulmer MG (1975) Phase relations in the ten-year cycle. *J Anim Ecol* 44:609–621
- Cortez M, Ellner S (2010) Understanding rapid evolution in predator–prey interactions using the theory of fast-slow dynamical systems. *Am Nat* 176:E109–E127
- Cousyn C, De Meester L, Colbourne JK, Brendonck L, Verschuren D, Volckaert F (2001) Rapid, local adaptation of zooplankton behavior to changes in predation pressure in the absence of neutral genetic changes. *Proc Natl Acad Sci USA* 98:6256–6260
- Dercole F, Ferriere R, Gragnani A, Rinaldi S (2006) Coevolution of slow-fast populations: evolutionary sliding, evolutionary pseudo-equilibria and complex Red Queen dynamics. *Proc R Soc B Biol Sci* 273:983–990
- Doebeli M, Koella JC (1995) Evolution of simple population-dynamics. *Proc R Soc Lond B Biol Sci* 260:119–125
- Doebeli M, Koella J (1996) Chaos and evolution. *Trends Ecol Evol* 11:220–220
- Dube D, Kim K, Alker AP, Harvell CD (2002) Size structure and geographic variation in chemical resistance of sea fan corals *Gorgonia ventalina* to a fungal pathogen. *Mar Ecol Prog Ser* 231:139–150
- Duffy MA, Sivars-Becker L (2007) Rapid evolution and ecological host–parasite dynamics. *Ecol Lett* 10:44–53
- Duffy MA, Hall SR (2008) Selective predation and rapid evolution can jointly dampen effects of virulent parasites on daphnia populations. *Am Nat* 171:499–510
- Duffy MA, Brassil CE, Hall SR, Tessier AJ, Caceres CE, Conner JK (2008) Parasite-mediated disruptive selection in a natural *Daphnia* population. *BMC Evol Biol* 8:80
- Duffy MA, Hall SR, Caceres CE, Ives AR (2009) Rapid evolution, seasonality, and the termination of parasite epidemics. *Ecology* 90:1441–1448
- Duncan AB, Little TJ (2007) Parasite-driven genetic change in a natural population of *Daphnia*. *Evolution* 61:796–803
- Ellner S, Turchin P (1995) Chaos in a noisy world—new methods and evidence from time-series analysis. *Am Nat* 145:343–375
- Ellner SP, Kendall BE, Wood SN, McCauley E, Briggs, CJ (1997) Inferring mechanism from time-series data: delay-differential equations. *Physica D* 110:182–194
- Ellner SP, Hairston NG Jr, Kearns CM, Babai D (1999) The roles of fluctuating selection and long-term diapause in microevolution of diapause timing in a freshwater copepod. *Evolution* 53:111–122
- Ellner SP, Seifu Y, Smith RH (2002) Fitting population dynamic models to time-series data by gradient matching. *Ecology* 83:2256–2270
- Ezard THG, Cote SD, Pelletier F (2009) Eco-evolutionary dynamics: disentangling phenotypic, environmental and population fluctuations. *Philos Trans R Soc B Biol Sci* 364:1491–1498
- Ferriere R, Fox GA (1995) Chaos and evolution. *Trends Ecol Evol* 10:480–485
- Fussmann GF, Loreau M, Abrams PA (2007) Eco-evolutionary dynamics of communities and ecosystems. *Funct Ecol* 21:465–477
- Gagneux S, Long CD, Small PM, Van T, Schoolnik GK, Bohannan BJM (2006) The competitive cost of antibiotic resistance in *Mycobacterium tuberculosis*. *Science* 312:1944–1946
- Grant PR, Grant BR (2002) Unpredictable evolution in a 30-year study of darwin’s finches. *Science* 296:707–711
- Hairston NG Jr, Walton WE (1986) Rapid evolution of a life-history trait. *Proc Natl Acad Sci USA* 83:4831–4833
- Hairston NG Jr, Lampert W, Caceres CE, Holtmeier CL, Weider LJ, Gaedke U, Fischer JM, Fox JA, Post DM (1999) Lake ecosystems—rapid evolution revealed by dormant eggs. *Nature* 401:446–446
- Hampton SE, Scheuerell MD, Schindler DE (2006) Coalescence in the Lake Washington story: Interaction strengths in a planktonic food web. *Limnol Oceanogr* 51:2042–2051

- Heath DD, Heath JW, Bryden CA, Johnson RM, Fox CW (2003) Rapid evolution of egg size in captive salmon. *Science* 299:1738–1740
- Hendry AP, Wenburg JK, Bentzen P, Volk EC, Quinn TP (2000) Rapid evolution of reproductive isolation in the wild: evidence from introduced salmon. *Science* 290:516–518
- Hooker G (2009) Forcing function diagnostics for nonlinear dynamics. *Biometrics* 65:928–936
- Ives AR, Carpenter SR, Dennis B (1999) Community interaction webs and zooplankton responses to planktivory manipulations. *Ecology* 80:1405–1421
- Ives AR, Dennis B, Cottingham KL, Carpenter SR (2003) Estimating community stability and ecological interactions from time-series data. *Ecol Monogr* 73:301–330
- Johst K, Doebeli M, Brandl R (1999) Evolution of complex dynamics in spatially structured populations. *Proc R Soc Lond B Biol Sci* 266:1147–1154
- Jones LE, Ellner SP (2004) Evolutionary tradeoff and equilibrium in an aquatic predator–prey system. *Bull Math Biol* 66:1547–1573
- Jones LE, Ellner SP (2007) Effects of rapid prey evolution on predator–prey cycles. *J Math Biol* 55:541–573
- Kassen R (2009) Toward a general theory of adaptive radiation: insights from microbial experimental evolution. *Year in evolutionary biology 2009*. *Ann NY Acad Sci* 1168: 3–22
- Kendall BE, Prendergast J, Bjornstad ON (1998) The macroecology of population dynamics: taxonomic and biogeographic patterns in population cycles. *Ecol Lett* 1:160–164
- Khibnik AI, Kondrashov AS (1997) Three mechanisms of Red Queen dynamics. *Proc R Soc Lond B Biol Sci* 264:1049–1056
- Kinnison M, Hairston NG Jr (2007) Eco-evolutionary conservation biology: contemporary evolution and the dynamics of persistence. *Funct Ecol* 21:444–454
- Kinnison MT, Unwin MJ, Quinn TP (2008) Eco-evolutionary vs habitat contributions to invasion in salmon: experimental evaluation in the wild. *Mol Ecol* 17:405–414
- Kondoh M (2007) Anti-predator defence and the complexity–stability relationship of food webs. *Proc R Soc B Biol Sci* 274:1617–1624
- Konishi S, Kitagawa G (2008) Information criteria and statistical modeling. *Springer Series in Statistics*, Springer, New York
- Levin SA (1972) Mathematical analysis of genetic feedback mechanism. *Am Nat* 106:145–164
- Levin SA, Udovic DJ (1977) Mathematical model of co-evolving populations. *Am Nat* 111:657–675
- Meyer JR, Ellner SP, Hairston NG Jr, Jones LE, Yoshida T (2006) Prey evolution on the time scale of predator–prey dynamics revealed by allele-specific quantitative PCR. *Proc Natl Acad Sci USA* 103:10690–10695
- Olsen EM, Heino M, Lilly GR, Morgan MJ, Brattey J, Ernande B, Dieckmann U (2004) Maturation trends indicative of rapid evolution preceded the collapse of northern cod. *Nature* 428:932–935
- Palkovacs EP, Marshall MC, Lamphere BA, Lynch BR, Weese DJ, Fraser DF, Reznick DN, Pringle CM, Kinnison MT (2009) Experimental evaluation of evolution and coevolution as agents of ecosystem change in Trinidadian streams. *Philos Trans R Soc B Biol Sci* 364:1617–1628
- Reznick DN, Ghalambor CK (2001) The population ecology of contemporary adaptations: what empirical studies reveal about the conditions that promote adaptive evolution. *Genetica* 112:183–198
- Reznick DN, Shaw FH, Rodd FH, Shaw RG (1997) Evaluation of the rate of evolution in natural populations of guppies (*Poecilia reticulata*). *Science* 275:1934–1937
- Shertzer KW, Ellner SP, Fussmann GF, Hairston NG Jr (2002) Predator–prey cycles in an aquatic microcosm: testing hypotheses of mechanism. *J Anim Ecol* 71:802–815
- Sinervo B, Svensson E, Comendant T (2000) Density cycles and an offspring quantity and quality game driven by natural selection. *Nature* 406:985–988
- Swain DP, Sinclair AF, Mark Hanson J (2007) Evolutionary response to size-selective mortality in an exploited fish population. *Proc R Soc Lond B Biol Sci* 274:1015–1022
- Swartz J, Bremermann H (1975) Discussion of parameter estimation in biological modelling: algorithms for estimation and evaluation of the estimates. *J Math Biol* 1:241–257
- Thompson JN (1998) Rapid evolution as an ecological process. *Trends Ecol Evol* 13:329–332
- Tien R (2010) Two theoretical studies investigating predator–prey interactions. PhD Thesis, Department of Ecology and Evolutionary Biology, Cornell University, Ithaca NY 14853
- Tyerman JG, Bertrand M, Spencer CC, Doebeli M (2008) Experimental demonstration of ecological character displacement. *BMC Evol Biol* 8:34
- Varah J (1982) A spline least squares method for numerical parameter estimation in differential equations. *SIAM J Sci Statist Comput* 3:28–46
- Weitz JS, Hartman H, Levin SA (2005) Co-evolutionary arms races between bacteria and bacteriophage. *Proc Natl Acad Sci USA* 102: 9535–9540
- Wootton JT, Emmerson M (2005) Measurement of interaction strength in nature. *Ann Rev Ecol Evol Syst* 36:419–444
- Yoshida T, Jones LE, Ellner SP, Fussmann GF, Hairston NJ Jr (2003) Rapid evolution drives ecological dynamics in a predator–prey system. *Nature* 424:303–306
- Yoshida T, Hairston NG Jr, Ellner SP (2004) Evolutionary trade-off between defence against grazing and competitive ability in a simple unicellular alga, *Chlorella vulgaris*. *Proc R Soc Lond B Biol Sci* 271:1947–1953
- Yoshida T, Ellner SP, Jones LE, Bohannan BJM, Lenski RE, Hairston NG Jr (2007) Cryptic population dynamics: Rapid evolution masks trophic interactions. *PLoS Biology* 5:1868–1879
- Zbinden M, Haag CR, Ebert D (2008) Experimental evolution of field populations of *Daphnia magna* in response to parasite treatment. *J Evol Biol* 21:1068–1078
- Zeineddine M, Jansen VAA (2005) The evolution of stability in a competitive system. *J Theor Biol* 236:208–215

Electronic Supplementary Material: Supplementary Appendix and Figures

Stephen P. Ellner¹ and Lutz Becks. Rapid prey evolution in response to two predators. *Theoretical Ecology*.
¹Corresponding author. Department of Ecology and Evolutionary Biology, Cornell University, Ithaca NY 14853-2701. spe2@cornell.edu

F Coexisting prey must be extreme types

Assume first that the set of possible algal clone types is a rectangle $p_* \leq p \leq p^*, \pi_* \leq \pi \leq \pi^*$. With two predators y and z (but it will be clear that the number of predators doesn't matter) the dynamics of algal clone i are of the form

$$\dot{x}_i = x_i \left[\frac{mS}{k(p_i, \pi_i) + S} - p_i y G - \pi_i z H - 1 \right] \quad (28)$$

where S is substrate availability, p_i and π_i are the palatabilities to the two predators, and G, H are the predators' grazing rates, which are functions of the algal densities. Time has been rescaled so that $\delta = 1$.

If (28) has reached an attractor with some set of coexisting algal clones, then each of those clones must have zero average per-capita rate of increase, where the average is taken over the attractor. That is, defining

$$W(p, \pi) = \left\langle \frac{mS}{k(p, \pi) + S} - pyG - \pi zH - 1 \right\rangle \quad (29)$$

where $\langle \bullet \rangle$ denotes the average of \bullet over the attractor, we must have $W(p_i, \pi_i) = 0$ for all coexisting types. Note that in (29) G and H are independent of p and π , because we are considering the increase of a rare invader and the grazing rates are set by the abundances and traits of the resident types. In order for the set of coexisting types to be non-invasible (i.e., in order for them to comprise an Evolutionarily Stable Coalition (ESC)), it must be the case that $W(p, \pi) < 0$ for any possible type (p, π) that is not in the ESC. Thus W must have a local maximum at each member of the ESC, with maximum value $W = 0$.

So if any ESC member has a trait whose value is in the interior of the set of possible values, the second derivative of W with respect to that trait value must be negative. Taking derivatives inside the angle-brackets (i.e., interchanging the order of differentiation and integration) we have

$$W'' = \left\langle \frac{(2(k')^2 - (k+S)k'') mS}{(k+S)^3} \right\rangle. \quad (30)$$

where $'$ and $''$ denote the first and second derivatives with respect to either p or π , and everything is evaluated at (p, π) . If k a linear function of p and π , then $k'' = 0$ so $W'' > 0$ everywhere. The only possible members of an ESC are the four corner genotypes. The same is true if k is concave down in both traits (i.e., $k'' < 0$): only corner types can belong to an ESC.

Alternatively, suppose that the defense levels are constrained to a tradeoff curve, such as the case of predator-specific incompatible defenses, so that $k = k(p), \pi = \pi(p)$. Then $W''(p)$ is given by (30) minus $\pi'' \langle zH \rangle$. So again a linear tradeoff will give $W'' > 0$ so that only extreme types can be in an ESC, so long as k is nonconstant. If k is constant, the same is true when $\pi'' < 0$, a nonlinear tradeoff such that (for example) $\pi(0.5) > \frac{1}{2}(\pi(0) + \pi(1))$, but a nonlinear tradeoff with $\pi'' > 0$ would favor intermediate types.

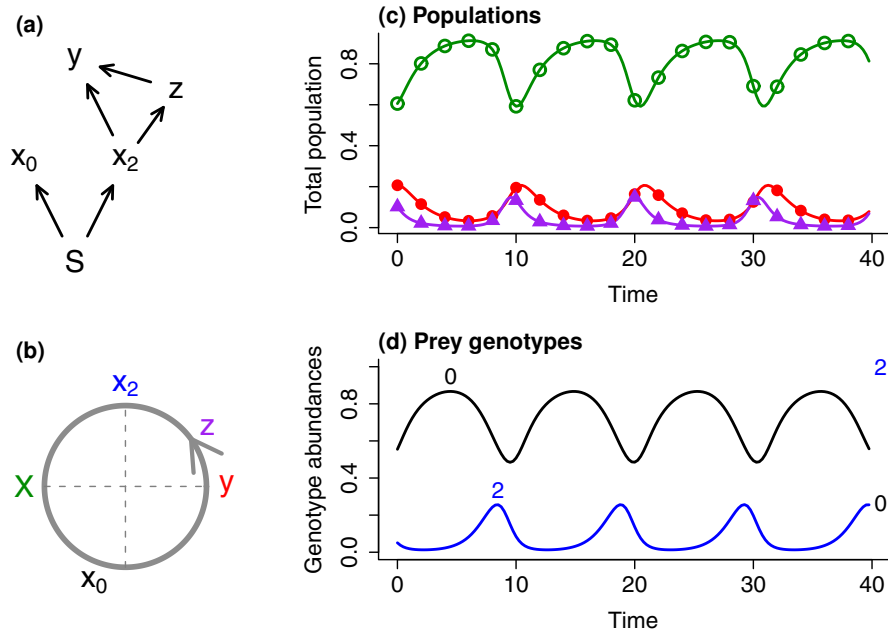


Fig. 13 Dynamics of the Intermediate Consumer model when one trait confers effective defense against both predators ($p_1 = 0.05, \pi_1 = 0.1$), presented as in Figure 2 in the main text

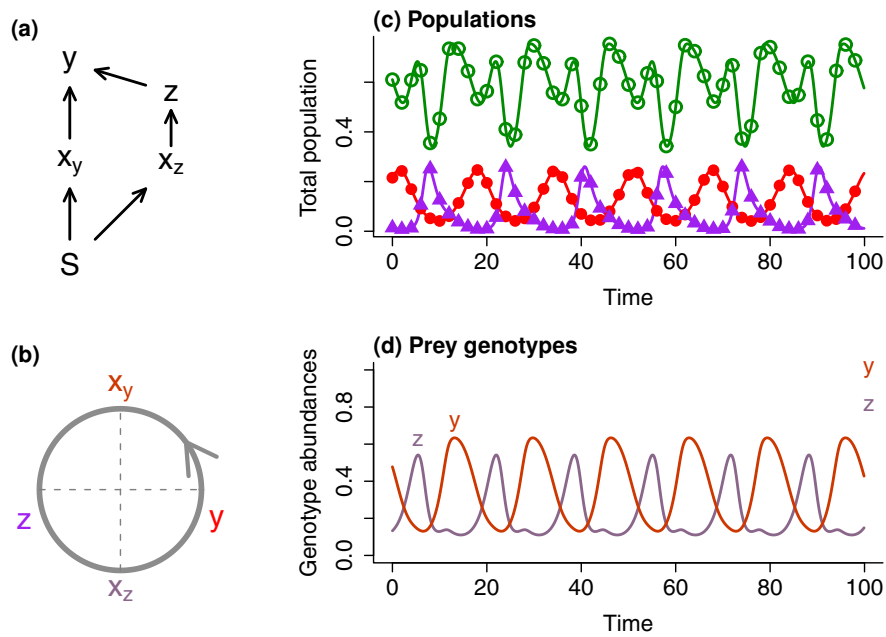


Fig. 14 Intermediate Consumer model dynamics with two prey genotypes having incompatible defenses, $\eta = 0.5, h = 4$

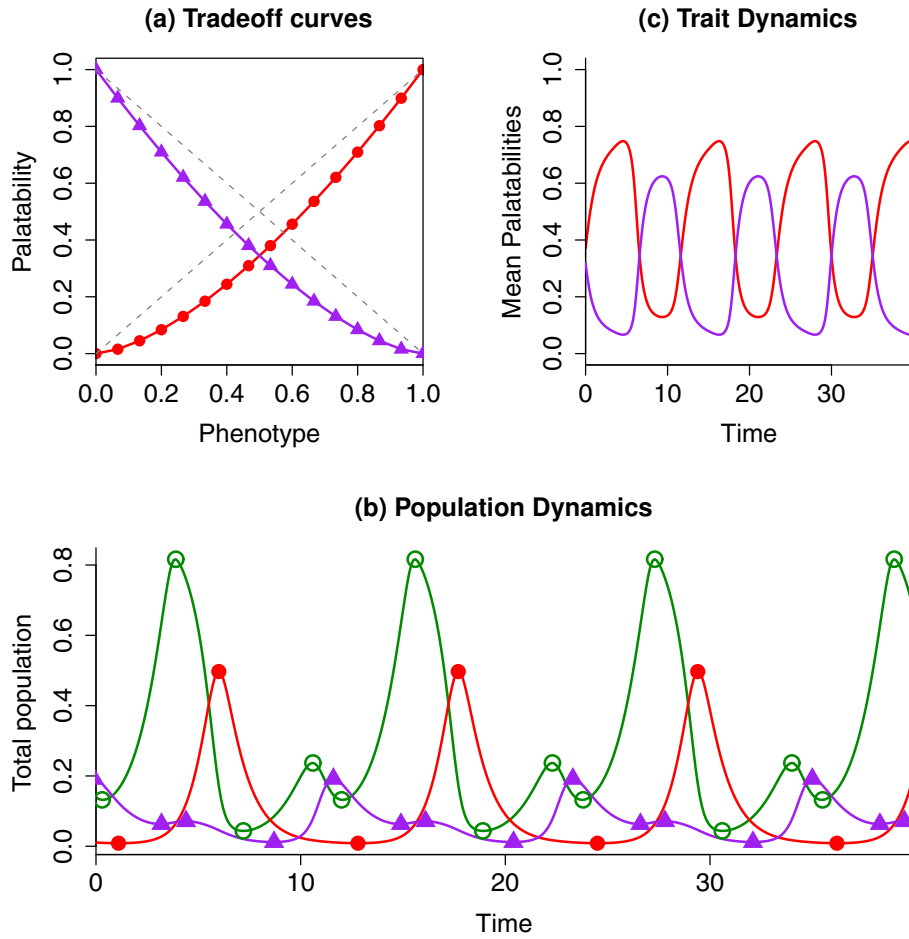


Fig. 15 An Intermediate Consumer model in which evolution is modeled by a gradient dynamics equation appropriate for a quantitative trait with relatively small additive genetic trait variance at any given time. (a) Tradeoff curves. Genotypes are characterized by a phenotype index $f \in (0, 1)$. The solid curves show the palatabilities to predators y (red, solid circles) and z (purple, solid triangles) as functions of f ; k was assumed to be the same for all genotypes. The dashed lines show a linear defense tradeoff. Intermediate f values are favored because they have low palatabilities to both predators. (b) Dynamics of the two predators (symbols as in panel (a)) and the prey populations (green, open circles). As in the clonal models with predator-specific incompatible defenses, the two predators oscillate out of phase with each other, and associated with each predator peak is a trough of the total prey population. (c) Trait dynamics. The curves show the palatabilities to both predators as a function of time. The model equations are

$$\begin{aligned}
 \dot{S} &= 1 - S - S \sum_i \frac{mx}{k+S} \\
 \dot{x} &= x \left[\frac{mS}{k+S} - \frac{gpy}{k_y+Q} - h\pi z - 1 \right] \\
 \dot{y} &= y \left[\frac{gQ}{k_y+Q} + \eta z - 1 \right] \\
 \dot{z} &= z [hR - \eta y - 1] \\
 \dot{f} &= Vf(1-f) \frac{p'(f)gy}{k_y+Q} - \pi'(f)hz
 \end{aligned} \tag{31}$$

with $Q = pX$, $R = \pi X$. Parameter values $m = 2$, $k = 0.03$, $g = 3$, $k_y = 0.2$, $\eta = 0.25$, $h = 20$, $V = 0.25$, palatability functions $p = (1 - f)^{1/a}$, $\pi = f^{1/a}$ with $a = 0.65$.

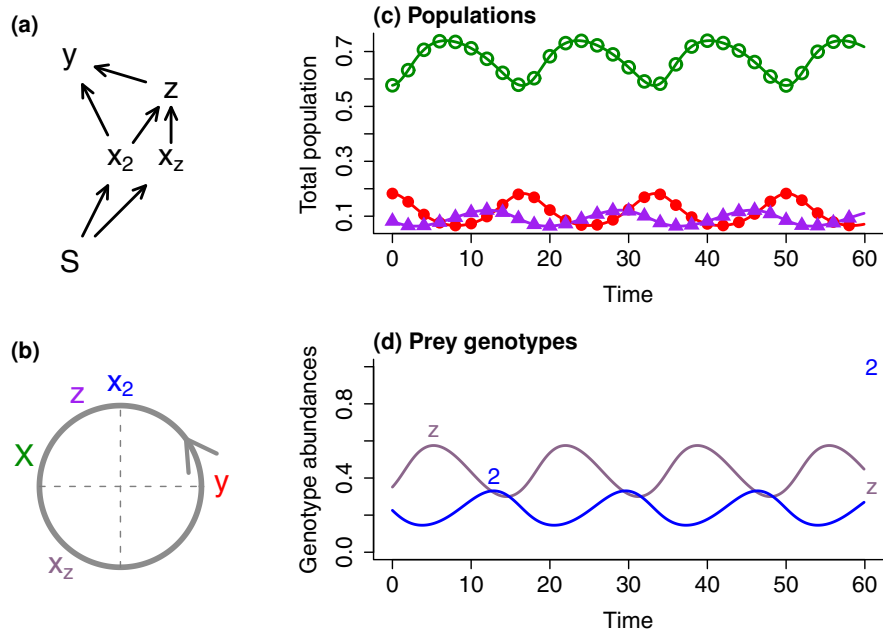


Fig. 16 Intermediate Consumer model dynamics when the ESC consists of the two prey types without defense against the intermediate predator z , and the $x \rightarrow z \rightarrow y$ chain is very weak ($h = 1.5$, $\eta = 0.05$).

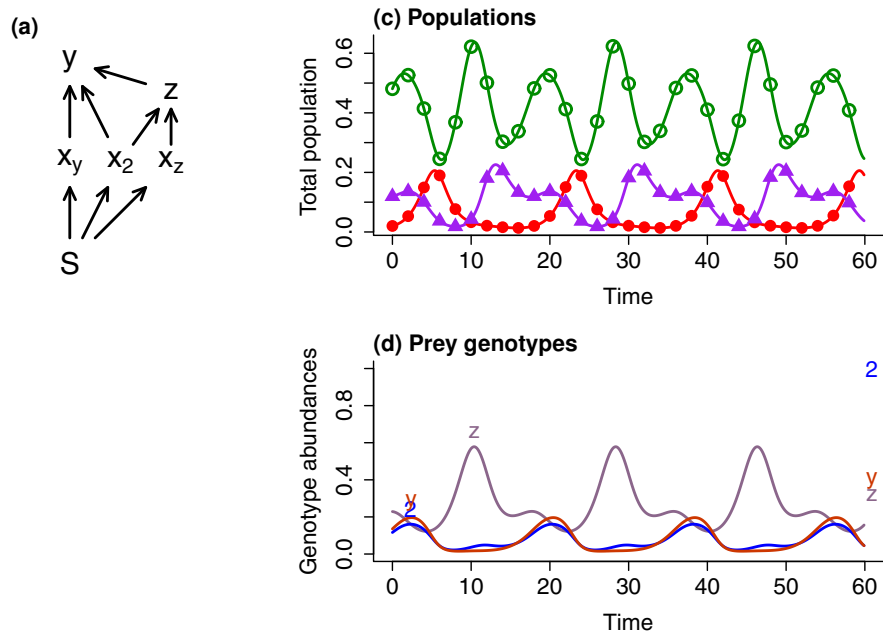


Fig. 17 Intermediate Consumer model dynamics when the ESC consists of the three prey types that are vulnerable to attack by at least one of the predators.

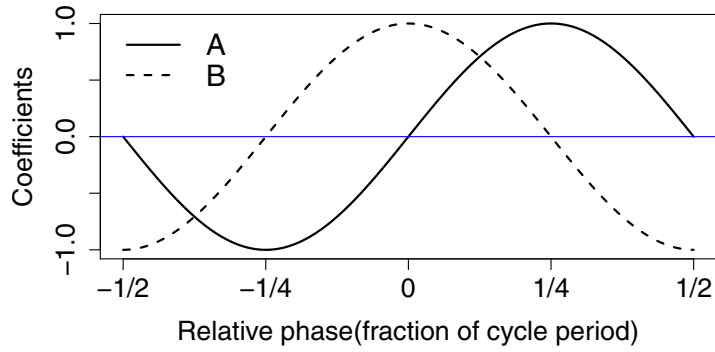


Fig. 18 Relationship between the coefficients A and B in equation (12), scaled so that $\sqrt{A^2+B^2} = 1$, and the phase of the forced variable relative to the forcing variable. A relative phase of $-1/4$, for example, means that the forced variable lags the forcing variable by a quarter of the cycle period

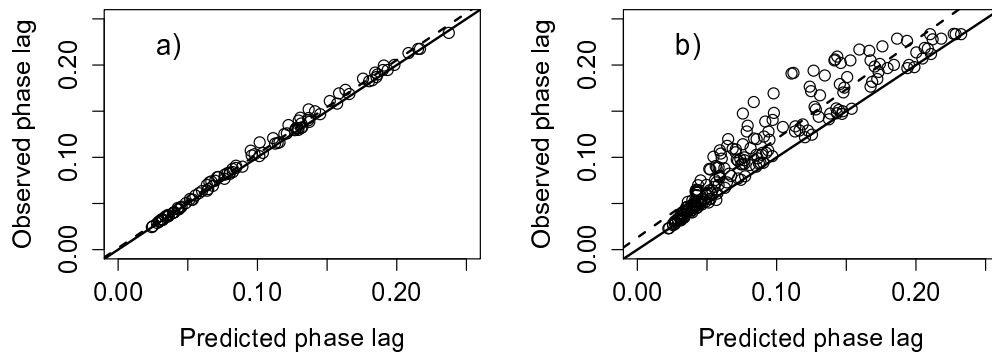


Fig. 19 Comparison of phase lag (between the focal prey species and the intermediate predator) observed in numerical simulations of (13) with the predicted lag (15). The solid line is the 1:1 line; the dashed line is the linear regression of observed on predicted phase lags. Numerical simulations were run with $\varepsilon = 0.1$ in panel (a), and $\varepsilon = 0.5$ in panel (b). Parameter value sets leading to positive values of \bar{z} and \bar{w} were generated randomly, as follows: $M \sim U(0, 10)$; $\phi \sim 1/M + U(0.05, 10)$; $h \sim U(0.05, 5)$; $\bar{x} \sim U(0.05/h, 0.95/h)$; $T \sim U(5, 50)$ where $U(a, b)$ denotes a uniform distribution on the interval $[a, b]$.